



Calhoun: The NPS Institutional Archive
DSpace Repository

Theses and Dissertations

1. Thesis and Dissertation Collection, all items

1989-09

A case study of Japanese coastal frontogenesis

Korcal, James H.

Monterey, California. Naval Postgraduate School

<http://hdl.handle.net/10945/25728>

This publication is a work of the U.S. Government as defined in Title 17, United States Code, Section 101. Copyright protection is not available for this work in the United States.

Downloaded from NPS Archive: Calhoun



<http://www.nps.edu/library>

Calhoun is the Naval Postgraduate School's public access digital repository for research materials and institutional publications created by the NPS community. Calhoun is named for Professor of Mathematics Guy K. Calhoun, NPS's first appointed -- and published -- scholarly author.

Dudley Knox Library / Naval Postgraduate School
411 Dyer Road / 1 University Circle
Monterey, California USA 93943

NAVAL POSTGRADUATE SCHOOL

Monterey, California



THESIS

K787

A CASE STUDY OF JAPANESE COASTAL
FRONTOGENESIS

by

James H. Kırçal

September 1989

Thesis Advisor

Wendell A. Nuss

Approved for public release; distribution is unlimited.

T245982

REPORT DOCUMENTATION PAGE

1a Report Security Classification Unclassified		1b Restrictive Markings	
2a Security Classification Authority		3 Distribution Availability of Report	
2b Declassification Downgrading Schedule		Approved for public release; distribution is unlimited.	
Performing Organization Report Number(s)		5 Monitoring Organization Report Number(s)	
4a Name of Performing Organization Naval Postgraduate School		6b Office Symbol (if applicable) 35	7a Name of Monitoring Organization Naval Postgraduate School
4c Address (city, state, and ZIP code) Monterey, CA 93943-5000		7b Address (city, state, and ZIP code) Monterey, CA 93943-5000	
4a Name of Funding Sponsoring Organization		8b Office Symbol (if applicable)	9 Procurement Instrument Identification Number
4c Address (city, state, and ZIP code)		10 Source of Funding Numbers	
		Program Element No	Project No Task No Work Unit Accession No

1 Title (Include security classification) **A CASE STUDY OF JAPANESE COASTAL FRONTOGENESIS**

2 Personal Author(s) **James H. Korcal**

3a Type of Report Master's Thesis	13b Time Covered From To	14 Date of Report (year, month, day) September 1989	15 Page Count 54
---------------------------------------------	-----------------------------	---------------------------------------------------------------	----------------------------

6 Supplementary Notation The views expressed in this thesis are those of the author and do not reflect the official policy or position of the Department of Defense or the U.S. Government.

7 Cosati Codes			18 Subject Terms (continue on reverse if necessary and identify by block number) Meteorology, Asian Coastal Cyclogenesis/Frontogenesis
Field	Group	Subgroup	

9 Abstract (continue on reverse if necessary and identify by block number)

Coastal frontogenesis, which has been extensively studied off the east coast of the United States, proves to be an operational forecasting problem as well as a possible link to explosive cyclogenesis. Similar conditions that produce coastal fronts along the U.S. coast also exist over the western North Pacific Ocean off the coast of Japan. However, few studies have examined the mesoscale coastal phenomena that precede Asian coastal cyclogenesis. Therefore, a synoptic and mesoscale analysis was completed for an area near Tokyo, Japan prior to a 23 March 1986 explosive cyclogenetical event. Synoptic-scale analyses fail to pick up the details of any possible coastal frontogenesis. Results from the mesoscale analyses indicate that convergence and frontogenesis begin along the coast 24 hours prior to the cyclogenesis. The coastal frontogenesis seems to begin just inland as discrete regions of frontogenesis and then move offshore as a more or less continuous feature just prior to the passage of the cyclone. Imagery from the Japanese GMS satellite supports the sequence of events suggested by the mesoscale analyses. However, future studies will need a more complete data network especially over the water to further characterize this mesoscale phenomenon.

20 Distribution Availability of Abstract <input checked="" type="checkbox"/> unclassified unlimited <input type="checkbox"/> same as report <input type="checkbox"/> DTIC users		21 Abstract Security Classification Unclassified	
22a Name of Responsible Individual Wendell A. Nuss		22b Telephone (include Area code) (408) 646-2044	22c Office Symbol 63Nu

Approved for public release; distribution is unlimited.

A Case Study of Japanese Coastal Frontogenesis

by

James H. Korcal
Lieutenant Commander, United States Navy
B.S., United States Naval Academy, 1979

Submitted in partial fulfillment of the
requirements for the degree of

MASTER OF SCIENCE IN METEOROLOGY AND OCEANOGRAPHY

from the

NAVAL POSTGRADUATE SCHOOL
September 1989

ABSTRACT

Coastal frontogenesis, which has been extensively studied off the east coast of the United States, proves to be an operational forecasting problem as well as a possible link to explosive cyclogenesis. Similar conditions that produce coastal fronts along the U.S. coast also exist over the western North Pacific Ocean off the coast of Japan. However, few studies have examined the mesoscale coastal phenomena that precede Asian coastal cyclogenesis. Therefore, a synoptic and mesoscale analysis was completed for an area near Tokyo, Japan prior to a 23 March 1986 explosive cyclogenetical event. Synoptic-scale analyses fail to pick up the details of any possible coastal frontogenesis. Results from the mesoscale analyses indicate that convergence and frontogenesis begin along the coast 24 hours prior to the cyclogenesis. The coastal frontogenesis seems to begin just inland as discrete regions of frontogenesis and then move offshore as a more or less continuous feature just prior to the passage of the cyclone. Imagery from the Japanese GMS satellite supports the sequence of events suggested by the mesoscale analyses. However, future studies will need a more complete data network especially over the water to further characterize this mesoscale phenomenon.

TABLE OF CONTENTS

I. INTRODUCTION	1
II. BACKGROUND	3
III. DATA DESCRIPTION AND GEOGRAPHIC SETTING	6
A. DATA	6
B. TOPOGRAPHIC FEATURES	8
IV. SYNOPTIC ANALYSIS	10
A. 0000 UTC 21 MARCH 1986	10
B. 1200 UTC 21 MARCH 1986	12
C. 0000 UTC 22 MARCH 1986	15
D. 1200 UTC 22 MARCH 1986	17
V. MESOSCALE ANALYSIS	19
A. 1200 UTC 21 MARCH 1986	19
B. 0000 UTC 22 MARCH 1986	26
C. 0600 UTC 22 MARCH 1986	33
D. 1200 UTC 22 MARCH 1986	36
E. SUMMARY	41
VI. CONCLUSIONS AND RECOMMENDATIONS	42
LIST OF REFERENCES	44
INITIAL DISTRIBUTION LIST	46

LIST OF FIGURES

Figure 1.	Location and major topography of case study	9
Figure 2.	0000 UTC 21 March 1986 JMA man-machine surface analysis	11
Figure 3.	0000 UTC 21 March 1986 300 mb analysis	11
Figure 4.	0000 UTC 21 March 1986 700 mb analysis	12
Figure 5.	1200 UTC 21 March 1986 JMA man-machine surface analysis	13
Figure 6.	1200 UTC 21 March 1986 700 mb analysis	14
Figure 7.	1200 UTC 21 March 1986 300 mb analysis	14
Figure 8.	0000 UTC 22 March 1986 JMA man-machine surface analysis	16
Figure 9.	0000 UTC 22 March 1986 300 mb analysis	16
Figure 10.	1200 UTC 22 March 1986 JMA man-machine surface analysis	18
Figure 11.	1200 UTC 22 March 1986 300 mb analysis	18
Figure 12.	1200 UTC 21 March 1986 GMS infrared satellite imagery	20
Figure 13.	1200 UTC 21 March 1986 mesoscale surface analysis	21
Figure 14.	1200 UTC 21 March 1986 rawinsonde for Tateno (47646)	22
Figure 15.	1200 UTC 21 March 1986 rawinsonde vertical cross section	23
Figure 16.	1200 UTC 21 March 1986 divergence computed from observed winds	25
Figure 17.	1200 UTC 21 March 1986 frontogenesis computed from observed winds	25
Figure 18.	0000 UTC 22 March 1986 GMS infrared satellite imagery.	27
Figure 19.	0000 UTC 22 March 1986 GMS visible satellite imagery.	28
Figure 20.	0000 UTC 22 March 1986 mesoscale surface analysis	29
Figure 21.	0000 UTC 22 March 1986 rawinsonde vertical cross section	30
Figure 22.	0000 UTC 22 March 1986 divergence computed from observed winds	31
Figure 23.	0000 UTC 22 March 1986 frontogenesis computed from observed winds	32
Figure 24.	0000 UTC 22 March 1986 synoptic-scale frontogenesis	32
Figure 25.	0600 UTC 22 March 1986 GMS infrared satellite imagery.	34
Figure 26.	0600 UTC 22 March 1986 GMS visible satellite imagery.	35
Figure 27.	1200 UTC 22 March 1986 GMS infrared satellite imagery.	37
Figure 28.	1200 UTC 22 March 1986 mesoscale surface analysis	38
Figure 29.	1200 UTC 22 March 1986 rawinsonde vertical cross section	39
Figure 30.	1200 UTC 22 March 1986 divergence computed from observed winds	40
Figure 31.	1200 UTC 22 March 1986 frontogenesis computed from observed winds	40

ACKNOWLEDGMENTS

I would like to extend my sincere thanks to Professor Wendell Nuss, not only his support of this study but also for his enthusiasm and patience in teaching meteorology. His insights have provided me with yet another angle at which to approach the atmospheric sciences. A special thanks goes to Professor Carlyle Wash for his critical review of this thesis. I would also like to thank Mr. Dennis Laws at FNOC for his assistance in obtaining the numerical data used in this study. Finally, I would like to thank my wife Akemi, daughter Christy and son Jeffrey for their love and support during the past two years even when school and the "thesis" took priority over activities they may have wished to do.

I. INTRODUCTION

A review of the following literature (Bosart *et al* 1972, Bosart 1975 and NCAR 1984) indicates that coastal fronts are typically intense mesoscale baroclinic zones approximately 200-600 km long and 50-100 km (NCAR 1984) in width that occur in the planetary boundary layer. Most often they have been documented in the winter months off the New England coast. They occur with an anticyclone to the north causing convergent flow along the coast with a synoptic scale-cyclone to the south. During their lifetime of 12-24 hours enhanced precipitation areas have been observed and their boundary often acts as a dividing line between frozen and non-frozen precipitation. They persist until the synoptic flow from the southern cyclone dominates the weather pattern in the area (Bosart *et al* 1972 and Bosart 1975). It is postulated that they are possible modifiers of the synoptic-scale low. Since they are a mesoscale feature their existence is often unresolved with current numerical models and, therefore, they present an operational forecasting problem (Bosart *et al.* 1972 and NCAR 1984).

The mesoscale circulation of the coastal front interacts with the overall synoptic pattern of the region throughout its life and may be influenced by jets and jet streaks (NCAR 1984). It has been shown that coastal fronts have been a predecessor to coastal cyclogenesis and ultimately explosive cyclogenesis. Bosart (1981) in his analysis of the Presidents' Day Snowstorm of 18-19 February 1979 found that the coastal front was of major importance. It steered the cyclone along the coast until a vigorous shortwave overtook the system and caused explosive deepening. Uccellini *et al.* (1984) also agrees with Bosart's conclusion in an another study of the same storm.

In the study of two Asian cyclones off the coast of Japan, Nuss and Kamikawa (1989) suggest that separate coastal and warm fronts existed in their 23 March 1986 case study prior to explosive cyclogenesis. This cyclone ultimately produced a unusually heavy snowfall in the Tokyo and the surrounding region, which includes four major U.S. military activities. The explosive event also disrupted maritime operations due to its proximity to major shipping lanes leading to and from Tokyo Bay. However, Nuss and Kamikawa conclude that their synoptic analysis was insufficient to resolve the coastal front prior to explosive cyclogenesis taking place.

Since the area east of Japan is the location of the frequency maximum of North Pacific Ocean explosive deepening (deepening of 1 mb h for 24 h) according to Sanders

and Gyakum (1980), and Gyakum *et al.* (1989), a case study of the coastal frontogenesis and events prior to the deepening of the 23 March case of Nuss and Kamikawa is conducted. It also will act as a ground truth for future conceptual and numerical models of the coastal front phenomena. Also, inconsistencies (discussed in the next section) as to how coastal features form, are found in U.S. Navy operational forecasters handbooks for the Kanto Plain and off-shore areas. Therefore, it is the purpose of this paper to discuss the structure and dynamics of the coastal front off Japan near the Kanto Plain, prior to the 23 March 1986 explosive event, in an attempt to further understand the coastal front phenomena. The area of the study will be referred to as the area of interest (AOI) for the remainder of the case study.

A survey of coastal fronts will be discussed in chapter two followed by a description of the data set utilized and topographic features of Japan in chapter three. Chapter four contains a synoptic analysis while chapter five analyzes the mesoscale features of the Japanese coastal front. Conclusions and recommendations follow in chapter six.

II. BACKGROUND

Coastal frontogenesis has been extensively studied off the east coast of the United States especially New England (Bosart *et al.* 1972, Bosart 1975, Marks and Austin 1979, Ballintine 1980 and NCAR 1984). East coast coastal fronts are most often observed with a cold anticyclone to the north of New England and a synoptic-scale developing low pressure system well to the south of the area of formation. It is a boundary layer phenomenon with differential friction setting up convergence and favorable deformation between modified easterly geostrophic flow over the water and a northerly flow inland, dammed against the Appalachian Mountains of New England. Bosart (1975) indicates that an initial temperature gradient is necessary if differential friction is to be effective in packing isotherms together in the formation of a frontal zone. Thermal contrasts as high as one degree centigrade per kilometer over 5-10 km have been observed on a length scale of approximately 100 km (Bosart *et al.* 1972).

Bosart (1975) concluded that geostrophic deformation itself is not capable of initiating a coastal front since the magnitude is much smaller than observed deformation in the vicinity of the coastal fronts studied. The standard synoptic-scale assumption that frontal winds satisfy geostrophic balance does not hold in the coastal front case where friction is the most important factor.

According to Bosart (1975), coastal fronts appear to have the greatest affinity for coastlines which curve anticyclonically when viewed from north to south, which would aid formation by topographically forcing confluence. Along with the New England coastlines, other areas of possible coastal frontogenesis are off the coast of the Carolinas and in the Gulf of Mexico along the Texas coast (Bosart 1975). Currently, the GALE (Genesis of Atlantic Lows Experiment) is investigating several cases of coastal frontogenesis off the North Carolina coast (GALE 1988).

Utilizing a numerical model with the terrain effects of New England incorporated, Ballintine (1980) concluded that the Appalachian Mountain Range plays a significant role in maintaining northerly flow inland from the coast due to its orientation. The northerly flow just inland from the coast over the nearly flat terrain was induced as long as the winds were from the northeast and a cold pool of air existed near the coast. They also show the importance of surface roughness in producing significant cross isobar flow at low levels.

Another important physical factor influencing the low-level winds according to Ballintine (1980) is the effect of heating from the ocean surface. As the air heats over the water, a pressure differential develops and causes the more northerly flow inland to be directed toward the coast amplifying convergence. This is analogous to the mesoscale land-sea breeze circulation. Latent heat release after precipitation has begun was also shown to back the winds to a more northerly direction west of the front. This was in response to an increase in cyclonic curvature along the frontal trough as more latent heat was released.

Coastal fronts have been observed to have many attributes of surface warm fronts including cyclonic wind shifts. They are often the dividing line between frozen and non-frozen precipitation. Also, increased observed precipitation on the coastal side indicates a thermally direct circulation, which cannot be explained utilizing only orographic effects (Bosart 1975).

To identify in greater detail the mesoscale precipitation features of coastal fronts, Marks and Austin (1979) studied six of Bosart's (1975) 57 coastal front cases that he analyzed in the period from 1964-72. These storms were selected for study because there was a significant amount of precipitation measured and adequate quantitative radar summaries were available. Their results support Bosart's conclusion that coastal fronts are locally induced low-level phenomena occurring well in advance of the cyclone and warm front to the south. They also show that coastal fronts produce local intensification of 20-50% of the associated large scale precipitation. Their hypothesis for intensification suggests that low clouds and fog are formed over the warm moist waters of the Gulf Stream and are lifted once they contact the shallow pool of cold air near the coastal front. Hydrometeors fall through the layer from above and grow by accretion thereby increasing precipitation at the surface. Marks and Austin also state that current observations are not detailed enough to verify or disprove their hypothesis.

In preliminary results from the GALE study, Riordan and Wang (GALE 1988) showed several unexpected features in a study of coastal frontogenesis off North Carolina. First, the coastal front did not form as a continuous band but rather as discrete bands propagating toward shore from across the Gulf Stream. In these bands, precipitation existed before being consolidated along the western boundary of the Gulf Stream at a later stage. Also, parallel zones of confluence and diffluence existed between the location of the front and the shoreline.

Little has been written about east Asia coastal cyclones (Chen and Dell'Osso 1987, and Nuss and Kamikawa 1989) and even less has been written about Asian coastal

frontogenesis. However, mention has been made of coastal phenomena in the form of lee troughs and thermally induced lows in local operational forecaster handbooks from U.S. Navy forecasters stationed in Yokosuka (1987) and Atsugi (1985) Japan. Both of these stations are within approximately 50 km of the Tokyo metropolitan area. The Yokosuka forecasters handbook refers to a lee trough (called an Oshima trough locally) produced offshore from the Tokyo area with the passage of a high pressure center over northern or central Honshu (main island of Japan). It also states that "...the orientation and axis of the lee trough vary considerably and these parameters cannot be forecast with an acceptable degree of accuracy".

The Atsugi forecaster handbook indicates that moderate to strong west to southwest flow along the mountains of southwest Japan form; lee depressions along the southern Japanese Alps, lee depressions along the coast and Kanto lows. The definition of a Kanto low itself being nebulous depending on which reference or person is consulted. However, a general definition based on personal experience and review of numerous publications would indicate that it is a mesoscale cyclonic circulation that forms in the Kanto (Tokyo) plain due to a combination of topographic, thermal and synoptic-scale effects.

As seen from the above discussion there is little information on Japanese/Asian coastal phenomena and what is available is somewhat conflicting for the operational forecaster. This case study will attempt to clarify the confusion and describe completely one Japanese mesoscale phenomenon.

III. DATA DESCRIPTION AND GEOGRAPHIC SETTING

A. DATA

Following Nuss and Kanikawa (1989), the gridded data set utilized in this case study is based on the C-analysis from the Japan Meteorological Agency (JMA). The C-analysis is optimally interpolated twice daily at 0000/1200 UTC in a polar stereographic projection to allow it to be easily overlayed with remapped imagery from the Japanese GMS geostationary satellite. The grid length is 254 km at 60° N and includes all data to 3.5 h after the stated map valid time.

In the synoptic-scale portion of this study (Chapter 4) four variables (V,T,Td,Z) are analyzed on selected levels from the surface to 300 mb at 0000/1200 UTC 21 and 22 March 1986. The C-analysis was then displayed in the NPS Interactive Digital Environmental Analysis (IDEA) computer laboratory utilizing graphics software developed at the National Center for Atmospheric Research (NCAR). The JMA man-machine surface analysis (JMA 1986) based on the C-analysis was also consulted in this portion of the study. Nuss and Kanikawa (1989) state that although the C-analysis incorporates potentially data sparse regions of the oceans, the close proximity of this cyclogenesis event to Japan places it in a relatively data rich region for synoptic-scale analyses. Therefore, it was felt that events occurring on the synoptic-scale were portrayed rather well by the C-analysis.

The mesoscale portion of the study (Chapter 5) utilizes the C-analysis as the first guess for an objective analysis field during the three primary synoptic times of 1200 UTC/21, 0000 UTC/22 and 1200 UTC/22 March 1986. The same four variables that are used in the synoptic-scale section are interpolated from the 254 km grid to a 15.875 km grid at the surface. Surface land and ship stations from Fleet Numerical Oceanography Center (FNOC) were then used to reanalyze the surface fields on this mesoscale grid in an attempt to study the mesoscale structure. The reanalysis was done using a Cressman objective analysis scheme (Cressman, 1959), which was run on the 15.875 km grid. Because upper levels did not have the same data density as the surface, the synoptic-scale gridded analyses will not have any mesoscale structure.

To increase confidence in the mesoscale gridded analyses, detailed hand analyses were completed at six-hour intervals from 1200 UTC 21 March to 1200 UTC 22 March 1986 from surface and ship observations contained in the FNOC data. To increase

confidence in the hand analyses, GMS satellite imagery were consulted and relied upon heavily in the data sparse oceanic portions of the analyses. The satellite imagery also provided time continuity between the analyses. Selected points of temperature, dewpoint and surface pressure were digitized from the hand surface analysis and used in the objective analysis to bring the hand analysis and computer analysis into closer agreement. Ship data that was obviously erroneous were deleted from the fields. No land synoptic reports were deleted. However, several had to have station pressure adjusted to sea level pressure utilizing the hypsometric equation. On this final modified grid, diagnostics were then run in an attempt to characterize the Japanese coastal front in the AOI.

The mesoscale portion of the study is limited by data resolution which was expected since routine data collection does not provide enough offshore observations for a mesoscale analysis of coastal phenomena. The sparsity of detailed surface observations was most apparent over the ocean in this study. However, lack of both land and ship data for the off-time synoptic analysis at 1800 UTC (0300 local) 21 March prevented the completion of a meaningful mesoscale analysis at that time. In addition, GMS imagery at 18 UTC 21 March was unavailable for analysis. Intermediate satellite imagery and more plentiful surface observations at 06 UTC/22 March were crucial in completing the mesoscale analysis at this time, which helped to maintain continuity between 00 12 UTC 22 March. Also unavailable were precipitation amount and radar summaries which can be helpful features in identifying coastal phenomenon as discussed in the background section. Although observational data were not as plentiful as one would hope for in a mesoscale study, the hand and numerically gridded analyses at the primary synoptic times corresponded very well with the excellent Japanese GMS infrared and visible satellite imagery.

Upper-air rawinsonde reports were used to construct vertical cross sections of equivalent potential temperature in the AOI utilizing GEMPAK software version 4.0 in the IDEA lab. Results corresponded well with numerical and hand analyses in spite of the large horizontal resolution between stations. Only seven stations (646, 654, 678, 778, 590, 600 and 971) were utilized in constructing cross sections. The last three stations were really not in the AOI but were used due to a software requirement that a minimum of four stations be utilized in the execution of the program.

B. TOPOGRAPHIC FEATURES

The volcanic islands of Japan are composed of some of the most rugged terrain in the world. Only one sixth of the Japanese Archipelago is arable due to its forested mountain ranges and variable terrain. The most significant mountain range is the Japanese Alps with an average elevation between 1500-3000 m (5000-12000 ft). The Alps run down the backbone of the main island of Honshu and are included in the area of interest for the case study (Fig. 1). Mt. Fuji, the highest point in Japan 3776m (12,395 ft) is also located in the AOI and lies approximately 75 km to the west-southwest of Tokyo (NOCD Atsugi, 1985).

Located at the bend or elbow of Honshu is the largest plain in Japan, the Kanto. The Kanto Plain comprises 13000 km (5000 sq mi) of flatlands and rolling hills. It also includes the highly populated and expensive real estate of Tokyo and its surrounding metropolitan areas (NOCD Atsugi, 1985).

Upon observing the coastline of Japan in the large scale section of Figure 1, one can make an analogy with the east coast of the United States off the Carolinas. Both curve anticyclonically when viewed from north to south with the elbow of the Kanto Plain (35° N) corresponding with the elbow of North Carolina-Cape Hatteras (36° N). This would seem to indicate that the coast of Japan in the AOI is conducive to coastal frontogenesis since Bosart (1975) states "Coastal fronts exhibited the greatest proximity for the region where the coastline curves anticyclonically as viewed from north to south". Another important physical feature according to Bosart *et al.* (1972) and Bosart (1975) is the presence of a coastal mountain range. Both coasts have significant coastal mountain ranges with the Japanese coast being more rugged. These coastal ranges act as a natural barrier and aid in setting up an increased thermal gradient between the land and the ocean. The warm Kuroshio and Gulf Stream currents which extend seaward to the northeast in the vicinity of the Kanto Plain and Cape Hatteras, respectively, also enhance the thermal gradient even further in these areas.

However, the coastline of Japan does differ from the Carolina coastline in that it is very rough and irregular in outline as seen in the enlarged (bottom) portion of (Fig. 1). There are three significant peninsulas and bays in the AOI with highly variable terrain superimposed with numerous smaller features. This would seem to indicate a tendency to increase the differential friction in the boundary layer which is important according to Bosart (1975) in packing the isotherms in this mesoscale feature. In short, the coast of Japan in the vicinity of 35° N possess the same physical attributes, possibly enhanced, for coastal frontogenesis as that of Cape Hatteras on the east coast of the United States.

IV. SYNOPTIC ANALYSIS

A. 0000 UTC 21 MARCH 1986

This case study focuses on coastal phenomena occurring along the Japanese coast near the Kanto Plain (AOI) between a non-explosive cyclone occurring on 19 March 1986 and an explosive event occurring on 23 March 1986 (Nuss and Kamikawa 1989). At 0000 UTC 21 March 1989 the non-explosive cyclone is approximately 300 n mi to the east of the northern most Japanese island of Hokkaido. The man-machine 0000 UTC 21 March JMA surface analysis (Fig. 2) shows high pressure beginning to ridge into Japan from a 1022 mb center located in northern China. The northern one-third of the country continues to be synoptically influenced by the non-explosive cyclone. Satellite imagery (not shown) indicates broken high clouds to be present along the east coast of Japan from 24° N to 27° N with multi-layered cloudiness over the northern portion of Honshu and Hokkaido. There is no evidence of a front in the AOI at this time. The winds in the AOI are westerly with Hachijojima (Fig. 1) reporting westerly winds at 270° at 15 kt.

Over the East China Sea near Taiwan a low pressure center, located on the polar front, is developing an inverted trough extending into the Yellow Sea. There is also significant baroclinicity along the coast of Japan extending to the Chinese coast in the vicinity of the inverted trough as evidenced by the packing of isotherms of equivalent potential temperature in the gridded surface analysis (not shown).

At upper levels the main synoptic feature is the non-explosive cyclone with a closed height center extending through the 300 mb level (Fig. 3). At the 700 mb level (Fig. 4) there is a significant short wave located over northern China just to the west of the Yellow Sea. There is also a slight indication of a short wave at 500 mb (not shown). On the 700 mb analysis there is a 20 m/s jet streak just west of Taiwan. The 300 mb analysis (Fig. 3) shows a significant 50 m/s jet streak that extends off the coast of China into the East China Sea with the left exit region located slightly to the north of the surface low. Wash *et al.* (1988) and many earlier authors indicate rapid deepening of cyclones occur when the left front region of the upper tropospheric jet is situated over the surface low. The upper level divergence enhances low-level convergence and deepens the low.

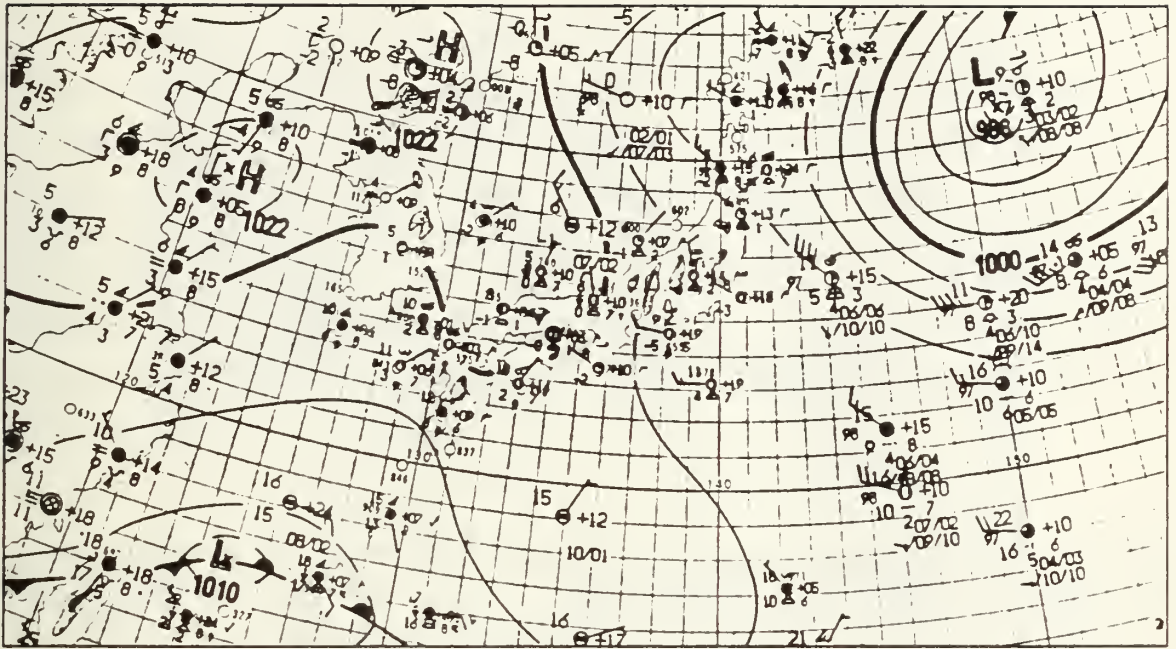


Figure 2. 0000 UTC 21 March 1986 JMA man-machine surface analysis with MSLP (mb). From JMA chart summaries.

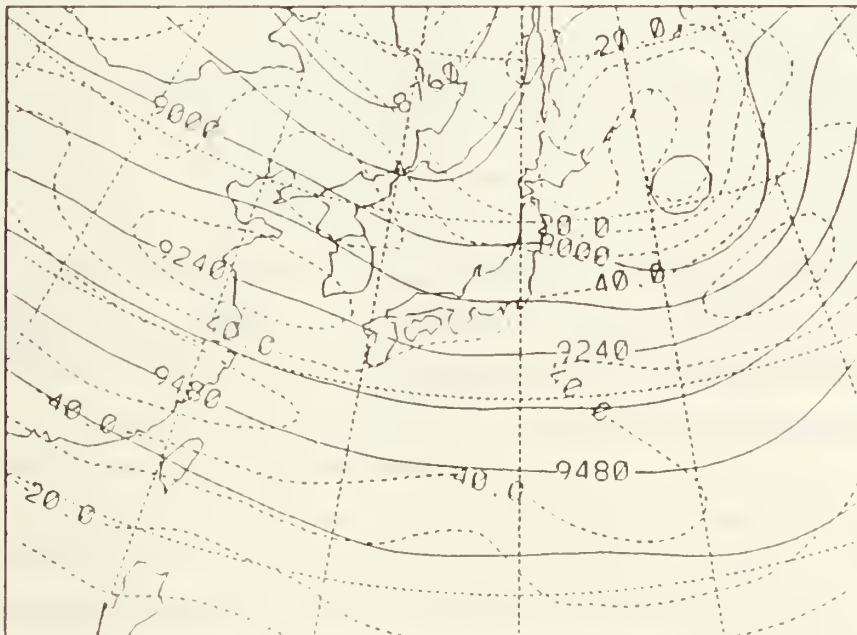


Figure 3. 0000 UTC 21 March 1986 300 mb analysis with heights (m, solid) and isotachs (m s, dashed).

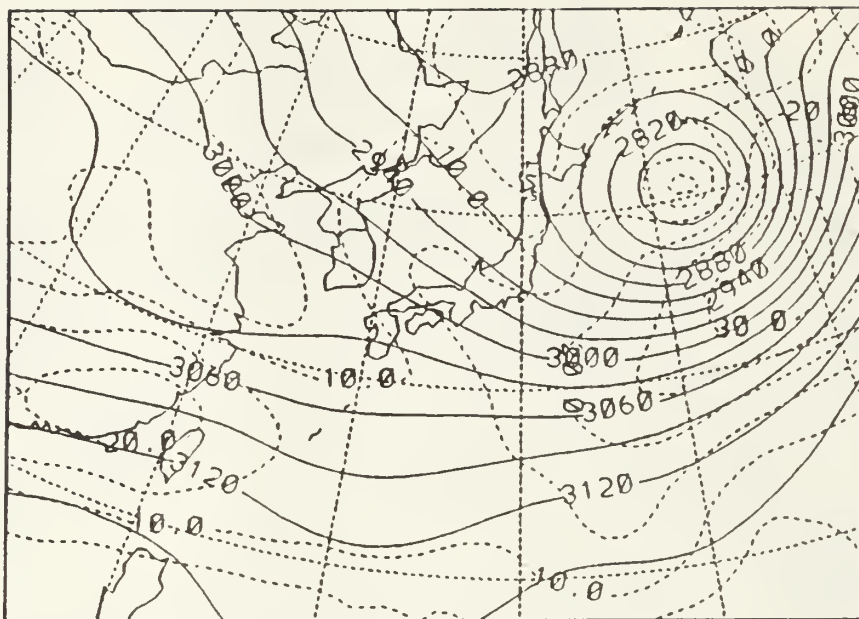


Figure 4. 0000 UTC 21 March 1986 700 mb analysis with heights (m, solid) and isotachs (m/s, dashed).

B. 1200 UTC 21 MARCH 1986

The surface JMA man-machine mix for 1200 UTC 21 March (Fig. 5) shows that the non-explosive low has moved further to the east-northeast and filled slightly. It is only effecting the northern island of Hokkaido. High pressure continues to push over most of Japan from a 1021 mb center now located in the Sea of Japan. A ridge axis is located north of the Kanto Plain extending southeastward over the North Pacific Ocean. Weak southeasterly flow around the ridge axis is producing weak shoreward winds at Hachijojima (130° @ 03 kt). This flow is possibly further enhanced under the influence of a weak high pressure center located to the southeast of Japan at 17° N, 148° E. A slight area of convergence is therefore conceivable along the coast since Omaezaki (47655) to the northwest of Hachijojima is reporting light winds out of the northwest (350° @ 04 kt). However, there is nothing to indicate a zone of convergence or front on the JMA surface analysis (Fig. 5) at this time. The low pressure center located along the polar front in the East China Sea has deepened two millibars since 0000 UTC. It continues to move to the northeast at seven knots.

At upper levels, the short wave at 700 mb (Fig. 6) has amplified over China and a slightly more significant short wave can be seen at 500 mb (not shown) from twelve

hours earlier. The jet streak at 700 mb near Taiwan has elongated and decreased in speed from 20 m/s to 15 m/s. A constant 50 m/s jet streak at 300 mb (Fig. 7) has also elongated north of Taiwan. The analysis is also attempting to show a 40 m/s jet streak over the north-central part of Japan with the southern boundary bisecting the AOI. As shown in later analysis by Nuss and Kamikawa (1989), the jet streak pattern at 300 mb is evolving into a potentially explosive situation. The southern jet streak with its divergent left exit region will be in a position to enhance the right entrance region of the northern jet as it swings down over central Honshu and the AOI creating maximum divergence aloft. Therefore, this particular upper level pattern should be carefully monitored operationally.

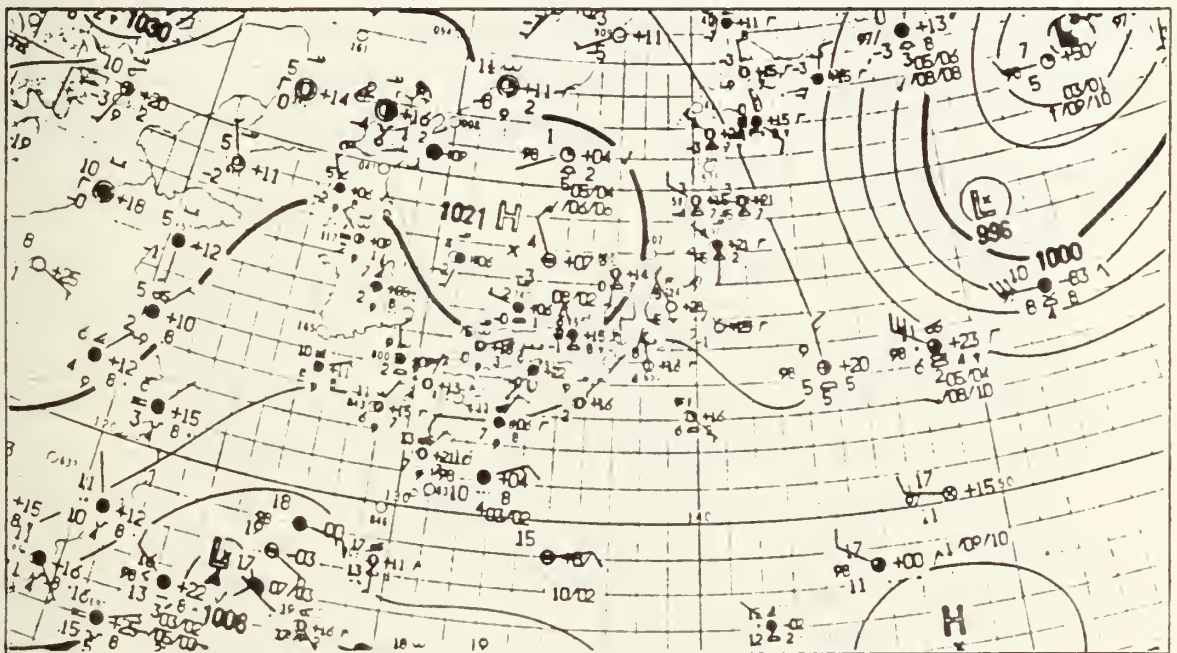


Figure 5. 1200 UTC 21 March 1986 JMA man-machine surface analysis with MSLP (mb). From JMA chart summaries.

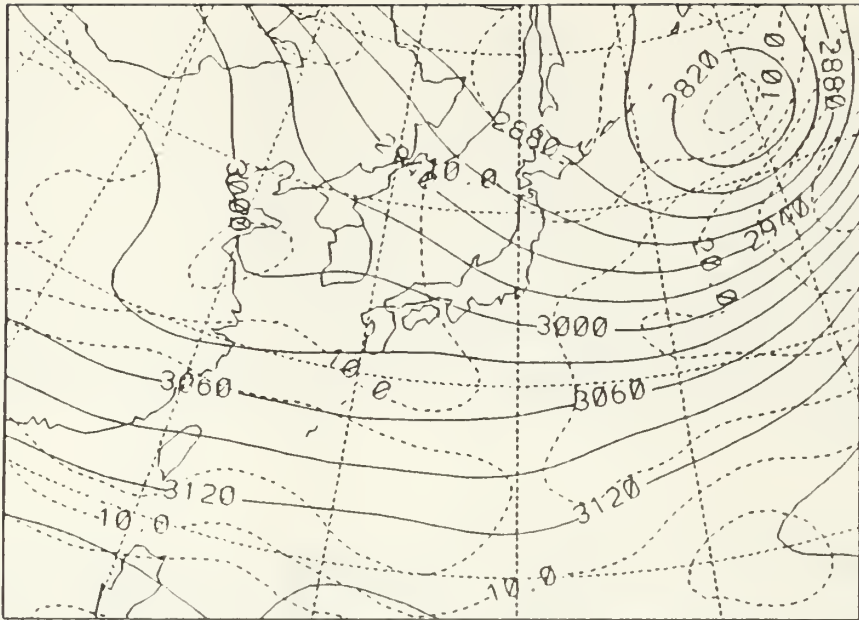


Figure 6. 1200 UTC 21 March 1986 700 mb analysis with heights (m, solid) and isotachs (m/s, dashed).

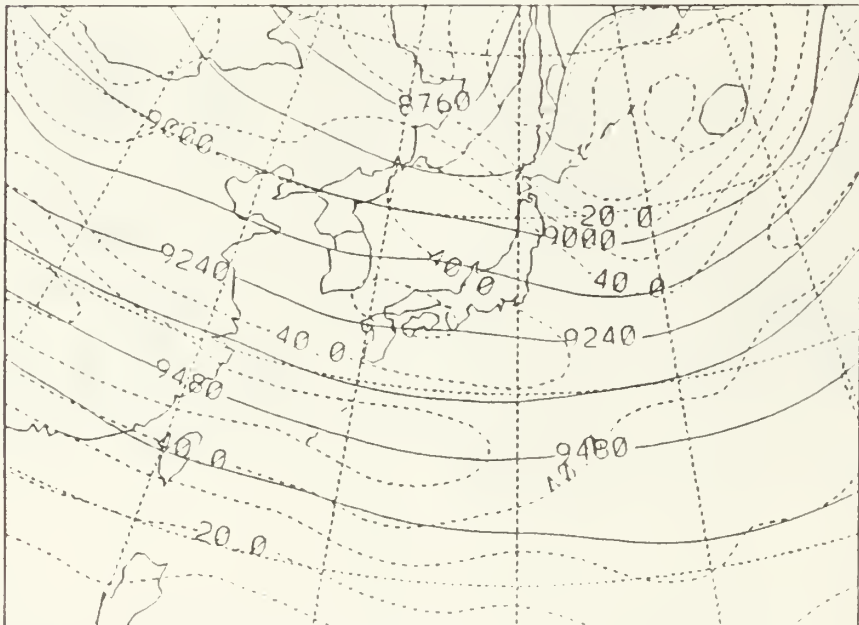


Figure 7. 1200 UTC 21 March 1986 300 mb analysis with heights (m, solid) and isotachs (m/s, dashed).

C. 0000 UTC 22 MARCH 1986

High pressure continues to dominate northern Japan on the JMA man-machine surface analysis (Fig. 8) with a 1021 mb center located along the west coast of northern Honshu. The ridge axis is in approximately the same position as twelve hours earlier and the flow around it is fairly geostrophic over the water with Hachijojima reporting winds at 120° at 11 kt. Along the coast, the frictional effects of the terrain have apparently forced more northerly winds at Omaezaki of 040° at 12 kt. This is the only evidence in the synoptic-scale analysis of convergence taking place in the AOI; it leads Nuss and Kamikawa (1989) to postulate frontogenesis in that area. However, once again the JMA surface analysis (Fig. 8) does not indicate any troughing or frontal activity in the AOI. Also, it is interesting to note that the weak high pressure area that had been at 17° N, 148° E on the 1200 UTC 21 March surface analysis (Fig. 5) is no longer present. It is assumed that it has been absorbed in the broad area of weak ridging occurring to the southeast of Japan and is possibly a cause of the increase in wind speed at the two stations mentioned above.

The cyclone along the polar front to the south of Japan continues to deepen slightly (2 mb) and is moving rather briskly to the north-northeast at approximately 17 kt. Another perturbation has also formed along the warm front to the east of the main cyclone and is currently located at 15° N, 143° E.

The upper-level features continue to support deepening of the cyclone with increases in wave amplitude at all levels and a westward tilt with height. The cyclone continues to be in a favorable location for upper-level divergence with respect to a jet streak running west to east from the Chinese coast as seen on the 300mb analysis (Fig. 9). The 40 m/s jet streak over central Honshu is also now oriented more east-west and is in a favorable location for increasing the divergence aloft as stated in Nuss and Kamikawa (1989). At this time it is questionable whether the divergence associated with this northern jet streak is interacting in any way with features in the AOI.

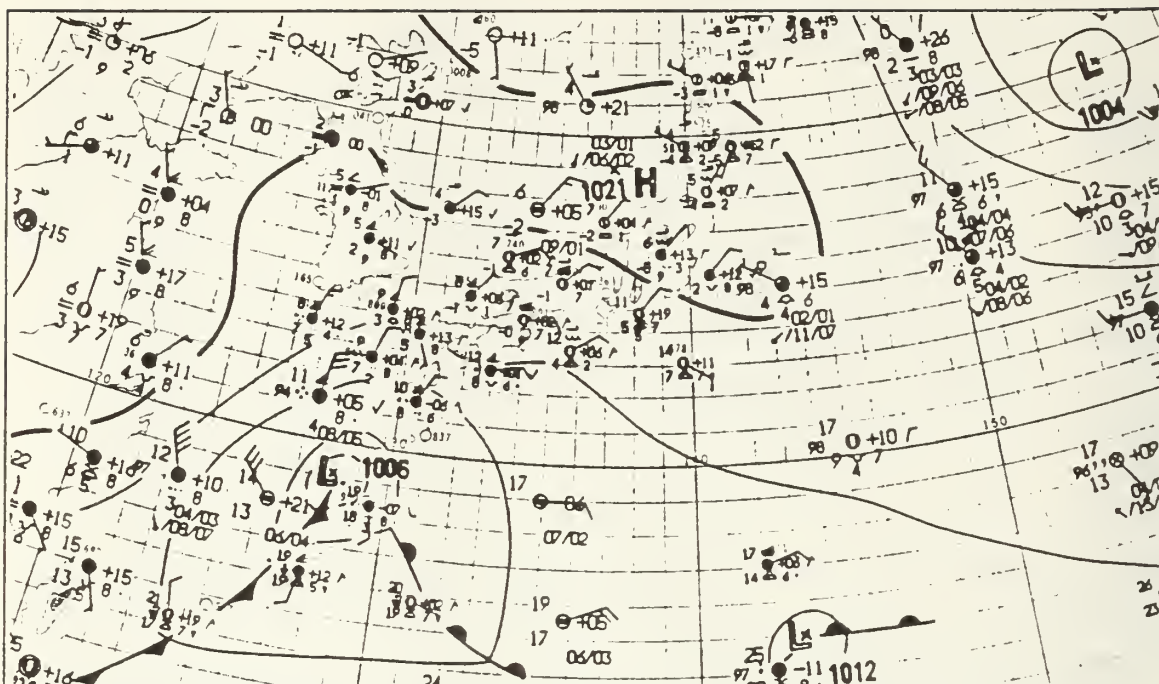


Figure 8. 0000 UTC 22 March 1986 JMA man-machine surface analysis with MSLP (mb). From JMA chart summaries.

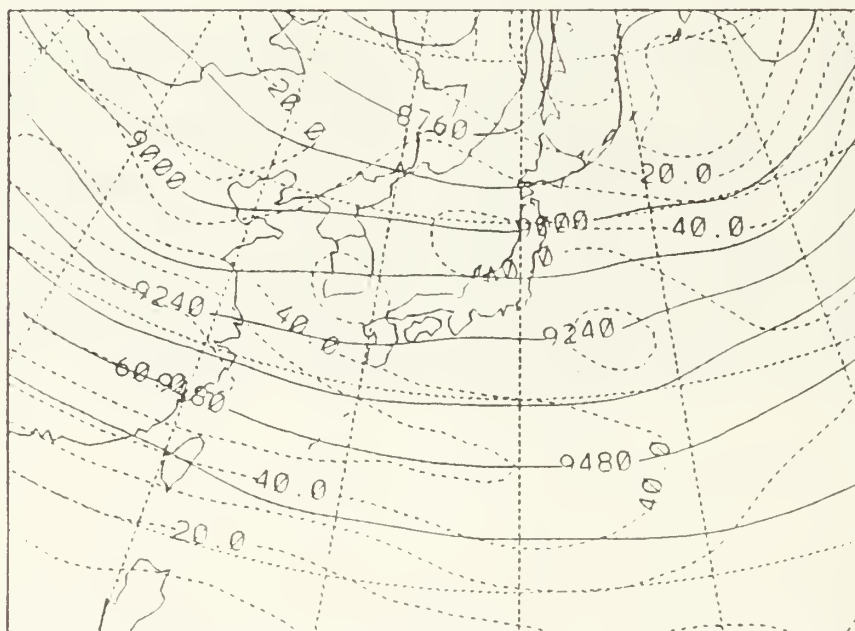


Figure 9. 0000 UTC 22 March 1986 300 mb analysis with heights (m, solid) and isotachs (m s, dashed).

D. 1200 UTC 22 MARCH 1986

High pressure continues to influence the northern half of Japan as shown on the JMA man-machine mix (Fig. 10) with the high pressure center (1024 mb) now located off the east coast of Japan in the North Pacific Ocean at 39° N, 146° E. The ridge axis has shifted slightly more to the northeast but flow over the water around the anticyclone continues to be nearly geostrophic with Hachijojima reporting winds of 130° at 11 kt. Along the coast, Omaezaki has winds from 040° at 17 kt, which are more nearly down gradient and indicate the frictional effects of the land mass once again. However, no troughing or frontal system is shown on the surface analysis (Fig. 10).

The synoptic-scale low pressure center along the polar front is still well to the south of the AOI. It has deepened 10 mb in the past twelve hours which qualifies it as a "bomb" according to Sanders and Gyakum (1980). It is still approximately 400 n mi southwest of Tokyo. Therefore, at its present speed of 15 kt it will take another 24 hours for cyclone passage in the AOI. The perturbation to the southeast of the major cyclone is now analyzed as a 1008 mb low.

At upper levels the synoptic-scale cyclone has good support with all levels indicating a westward tilt of the wave with height. It is also located under the left exit region of the jet streak at 300 mb (Fig. 11) emanating from the Chinese coast. This will definitely enhance the divergence aloft over the cyclone and continue to deepen it at the surface. The 40 m/s jet streak over central Honshu has moved slightly to the north and it is still unclear whether the divergent right entrance region is effecting the AOI.

Overall, the synoptic-scale overview has hinted at the possibility of some sort of convergence taking place in the AOI prior to the explosive cyclogenesis. This was done by comparing surface wind plots only; no definitive fronts or troughs were shown on any surface charts. It appears that a synoptic-scale chart does not have the resolution to pick up possible coastal phenomenon in the AOI.

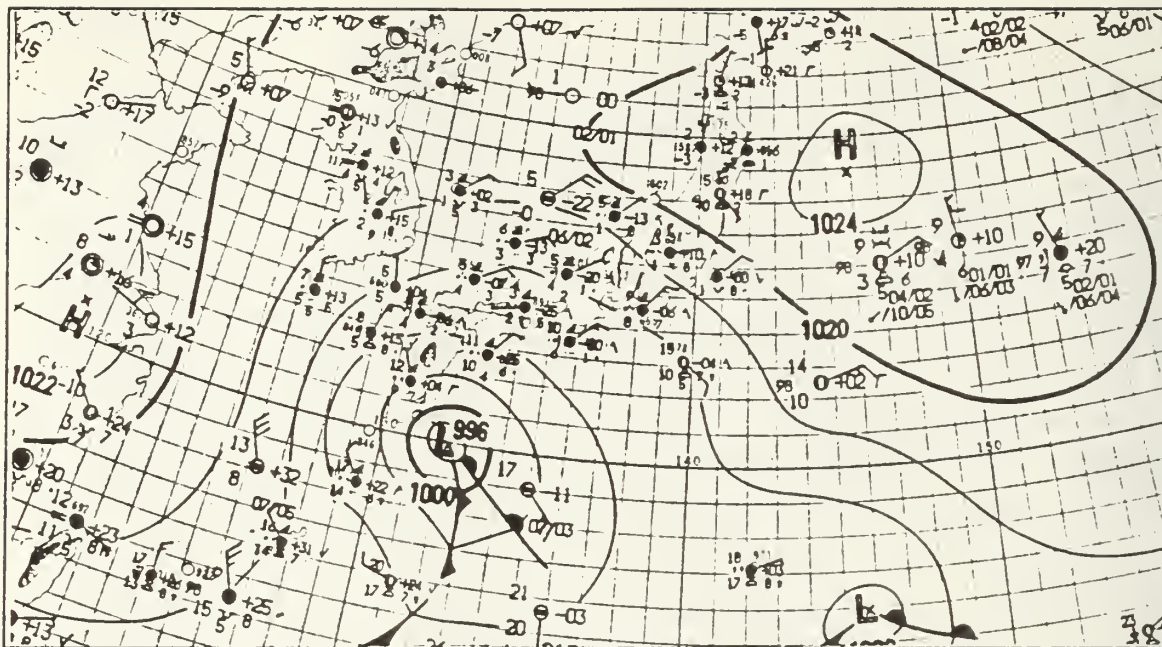


Figure 10. 1200 UTC 22 March 1986 JMA man-machine surface analysis with MSLP (mb). From JMA chart summaries.

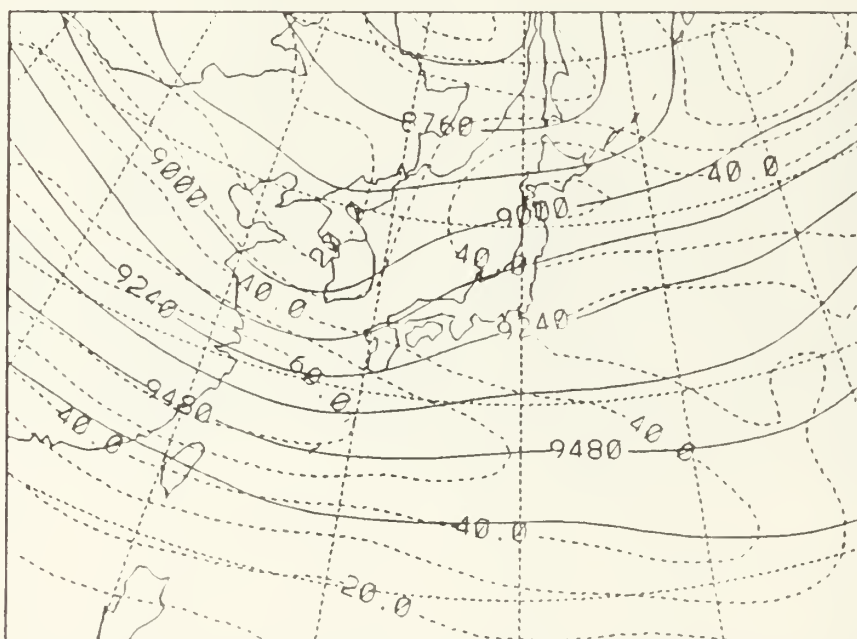


Figure 11. 1200 UTC 22 March 1986 300 mb analysis with heights (m, solid) and isotachs (m/s, dashed).

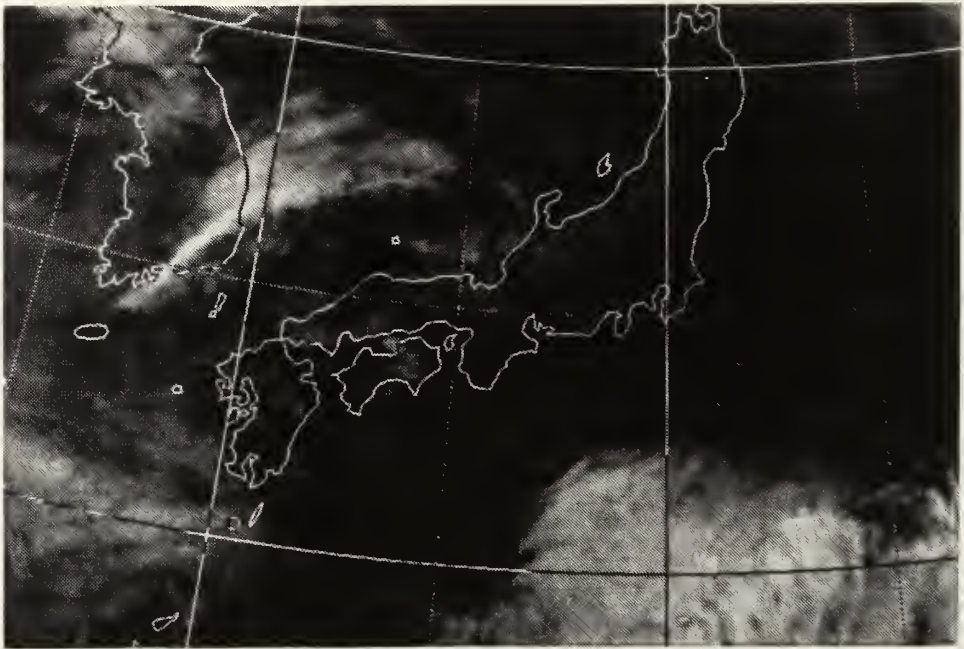
V. MESOSCALE ANALYSIS

A. 1200 UTC 21 MARCH 1986

One would expect from the JMA surface analysis at 1200 UTC 21 March (Fig. 5) that most of the east coast of central Honshu would be clear of clouds since it is under the influence of a high pressure center whose ridge is extending from the Sea of Japan. This is true in part with Japanese GMS infrared satellite imagery (Fig. 12a) showing clear areas along the coast north and south of the AOI. However, from south of the Izu Peninsula (Fig. 1) northward through the Tokyo Bay a circular mass of low clouds is present along the coast extending into the southern portion of the Kanto Plain, which suggests weak convergence along the coast. The position of these clouds can be seen easier in an enlarged image on Figure 12b. Upon comparing the satellite imagery with the topography of the AOI (Fig. 1) one can see that there is a sharp delineation of clouds caused by the topography of Honshu. The synoptic-scale flow created by the high in the Sea of Japan (Fig. 5) is being blocked by the Japanese Alps causing convergence along the western coast while there are coastal clouds occurring in the AOI along the east coast.

The modified mesoscale surface analysis (Fig. 13) shows fairly intense thermal packing along the coast in the AOI. The coldest air follows the topography of central Japan from north to south in the temperature analysis. Cold drainage winds indicated by the northwesterly winds over the mountains may be adding to the thermal contrast along the coast. Cold air, which has been depressed farthest to the south along the east coast of Japan where there is less blockage by the mountains, can be seen clearly as a cold tongue along the Boso Peninsula. The sounding at Tateno (Fig. 14) which is just to the north of Tokyo shows slight cold air advection indicated by backing winds with height. It is occurring below approximately 950 mb and weak warm air advection occurring above, which supports the idea of a low-level cold outflow in the Kanto region. There is a 20 kt wind maximum over Tateno from the east at the 950 mb level, which may be indicative of a low level jet. No evidence of this jet can be found at Hachijojima, which is 180 n mi to the south and is the nearest offshore rawinsonde station. The spacing between these stations fails to capture this feature. However, a vertical cross section of rawinsonde stations (Fig. 15) running north to south indicates a frontal zone between Tateno and Hachijojima as shown by a stratified layer and temperature gradient

a



b



Figure 12. 1200 UTC 21 March 1986 GMS infrared satellite imagery of: (a) Japanese Islands and adjacent seas, excluding Hokkaido and (b) enlarged view of the case study area.

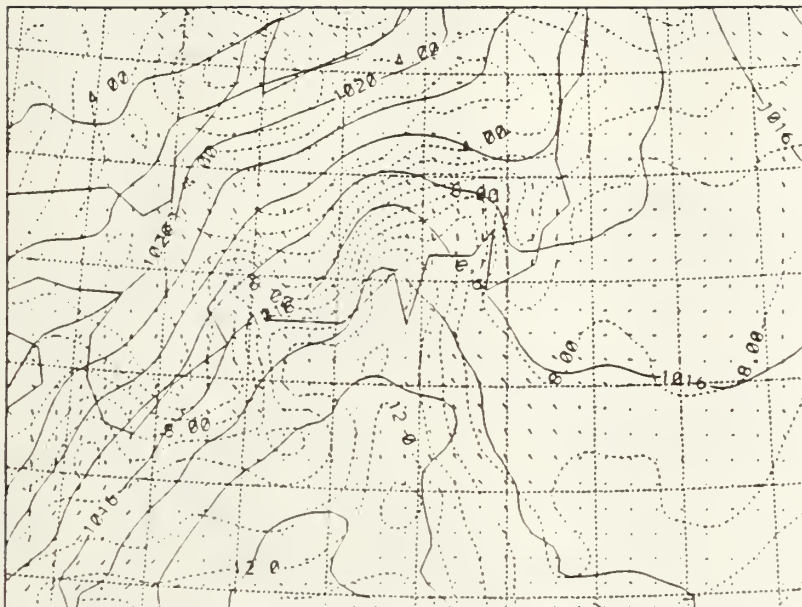


Figure 13. 1200 UTC 21 March 1986 mesoscale surface analysis with MSLP (mb, dashed), isotherms ($^{\circ}$ C , dashed) and wind (kt, arrows).

between the two stations. The layer is capped over Tateno at approximately 700 mb by a moderate inversion. Lines of constant mixing ratio that were hand drawn (not shown) show warm moist air from the east is indeed overriding a colder shallower pool of air at the surface. A further indication of the cold air advection in the area is evident in the IR satellite imagery (Fig. 12) just south of the Boso Peninsula. There is an apparent small scale low-level cyclonic circulation with a tail of cloudiness extending back along the north-south thermal gradient in Figure 13 to the main convergent area along the coast. This suggests that as the cold drier air is advected over the water by the weak anticyclonic flow, low clouds have formed where it is overrunning the warmer SST gradient of the Kuroshio current.

Examining the winds in Figure 13, there is northerly flow along the coast and inland against the Japanese Alps while the flow over the water is from the southeast. Apparently, frictional effects acting on the anticyclonic circulation in the boundary layer over the land has produced the nearly downgradient flow while over the water the flow is more nearly geostrophic. As a result, cold dry air (cloud free) is being advected into the AOI from the north while warm moist air (cloudy) is being advected in from the east over the warm Kuroshio current. This in turn is setting up an area of favorable shoreline

convergence in the AOI in a region of differential thermal stratification which was also seen in Bosart *et al.* (1972) and Bosart (1975) in studies along the New England coast.

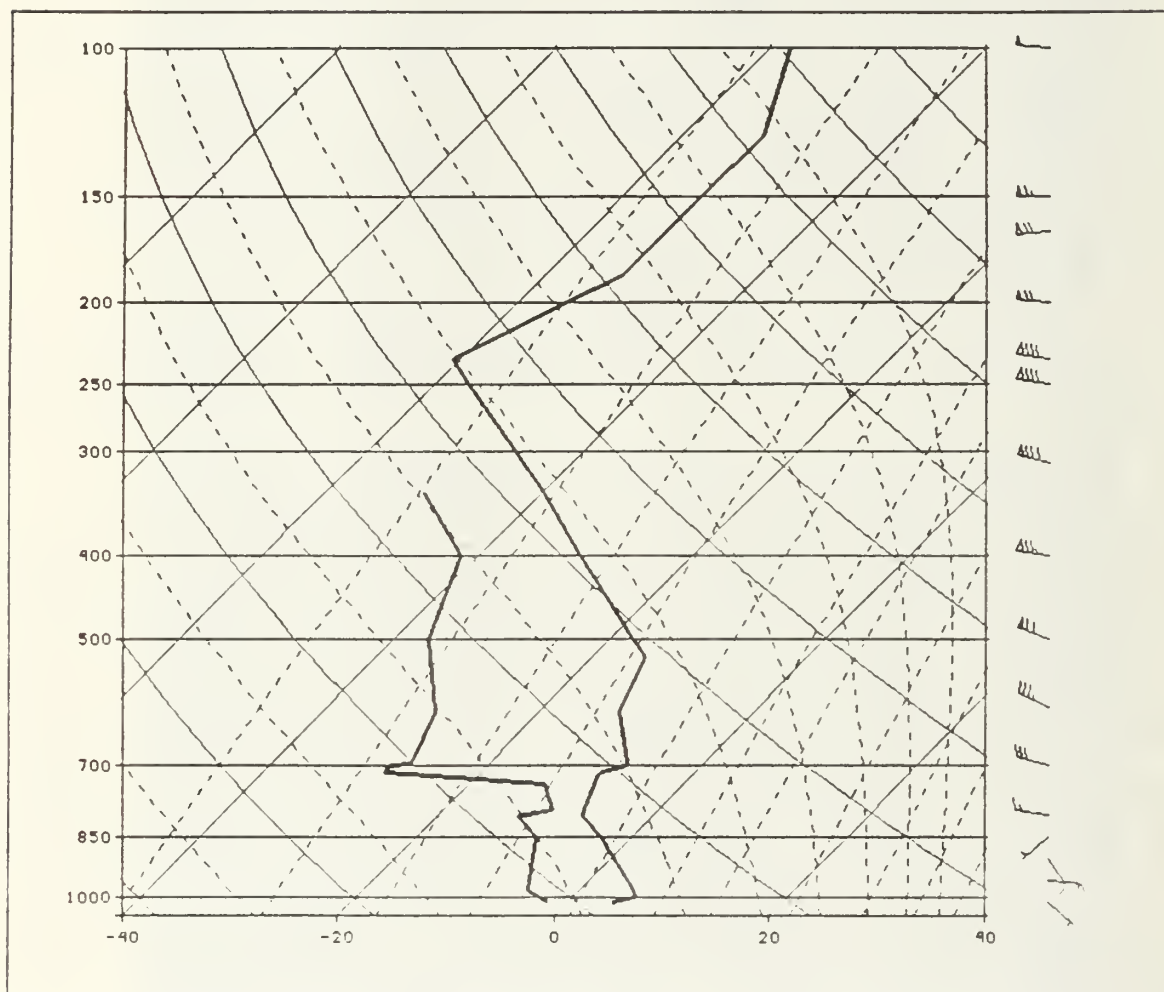


Figure 14. 1200 UTC 21 March 1986 rawinsonde for Tateno (47646) with temperature ($^{\circ}$ C , solid) and wind (kt, barbs).

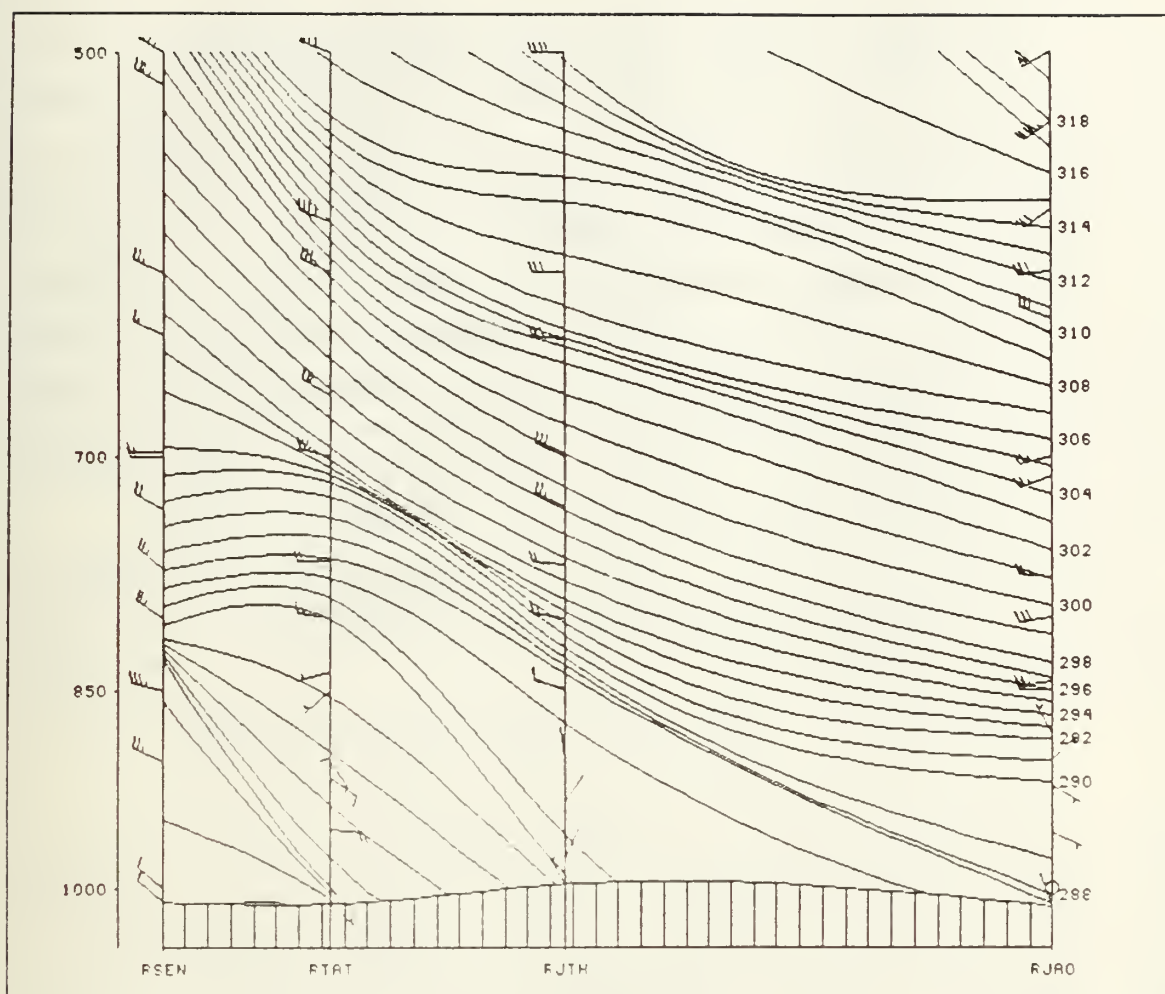


Figure 15. 1200 UTC 21 March 1986 rawinsonde vertical cross section with potential temperature (K, solid) and wind (kt, barbs). From left to right (north to south) Sendai (47590), Tateno (47646), Hachijojima (47678) and Chichijima (47971).

Divergence and convergence, which was computed from the gridded data set with observed winds, support this idea. A broad area of convergence (Fig. 16) is indicated along the coast within the AOI with a maximum of $-11.8 \times 10^{-5} \text{ s}^{-1}$ occurring just outside Tokyo Bay. This compares with Bosart's (1975) values of -8 to $-12 \times 10^{-5} \text{ s}^{-1}$ in the early stages of a coastal front off New England. Comparisons of numerical values are difficult between Bosart's case studies and this one since the time span of the coastal phenomena differ as well as the data resolution used to calculate the diagnostics. However, locations of major centers can be compared with respect to the coastal phenomena.

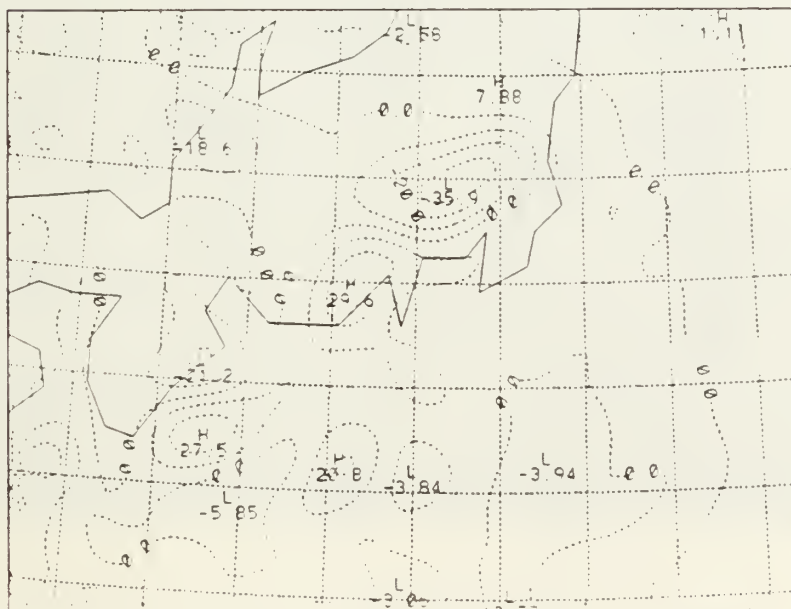
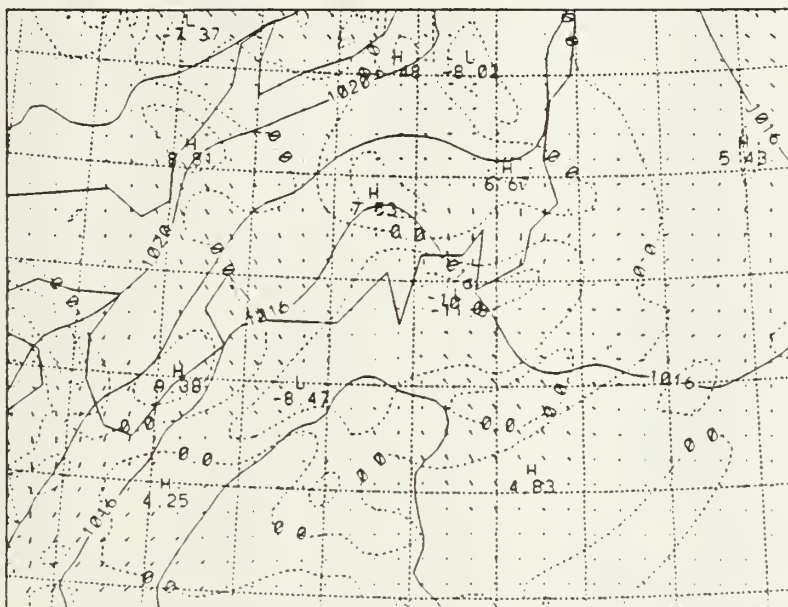
Precipitation is not being recorded at this time in the AOI. However, at 1500 UTC 21 March 1986, Oshima Island just outside of Tokyo Bay reported showers of rain during the past hour but not at the time of observation. This would support the occurrence of boundary layer instability in the area supporting the convergence analysis (Fig. 16) at 1200 UTC. It also supports the frontal analysis as depicted on the vertical cross section (Fig. 15) and a possible thermally direct circulation associated with the front.

Troughing is indicated up the bays along the east coast of Honshu on the mesoscale surface analysis (Fig. 13) which would seem to help in confirming that there is convergence occurring in the area. This troughing up the bays would agree with the Riordan and Wang (GALE 1988) preliminary results showing the coastal front as discrete bands vice being one continuous zone. This may be caused by the highly variable and rough terrain of the Japanese coastline creating mesoscale flows around the terrain.

Bosart (1975) also shows that the greatest observed deformation occurs along the coastal front. In order for a comparison to be made, frontogenesis was calculated using Newton's (1954) frontogenesis equation:

$$\frac{d}{dt} \left(-\frac{\partial \theta}{\partial y} \right) = -\frac{\partial}{\partial y} \left(\frac{\partial \theta}{\partial t} \right) + \frac{\partial u}{\partial y} \frac{\partial \theta}{\partial x} + \frac{\partial v}{\partial y} \frac{\partial \theta}{\partial y} + \frac{\partial w}{\partial y} \frac{\partial \theta}{\partial z}$$

However, the diabatic term (first) was deleted in calculations due to the lack of an adequate sea-surface temperature analysis (not shown). Therefore, the horizontal shear (second term) and vertical deformation (term three) were left as an approximation to observed deformation. The tilting term (four) which involves vertical motion is zero at the surface so is also not calculated. Frontogenesis calculated with observed winds (Fig. 17) did, in fact, correspond fairly well with convergence (Fig. 16) although the frontogenetical area did extend further down the coast. The maximum value occurred just south of the Izu Peninsula, which correlates with the cloud pattern on the satellite imagery. Calculation of terms two and three individually (not shown) show good correlation spatially with the deformation (convergence) term being several orders of magnitude greater than the horizontal shear term. This supports the interpretation of a significant ageostrophic contribution to the frontogenesis.



B. 0000 UTC 22 MARCH 1986

A very interesting pair of GMS infrared (Fig. 18) and visible (Fig. 19) imagery shows that over the past twelve hours the cloud mass has increased significantly in size and is occupying most of the AOI. The figures show a northeast to southwest line of high clouds with a distinct shadow line (visible) clearly seen to the northwest within a nearly circular mass of low clouds conforming roughly to the topography over the land area. This line of high clouds runs through the heart of Tokyo and suggests upward motion in the area. There is also a low cloud mass (34° N, 142° E) to the southeast of the major one with a distinct delineation along its eastern boundary suggesting colder air flow over warmer water as also seen at 1200 UTC 21 March. A thin cloud band running north-south along the maximum air temperature gradient is still present from twelve hours earlier. The satellite imagery also shows that the features occurring in and around the AOI are definitely separated from the synoptic-scale cyclone to the south.

The modified mesoscale surface analysis (Fig. 20) continues to indicate zones of troughing up each of the bays and out along the coast with major troughing occurring between Oshima and Hachijojima. The main thermal gradient has intensified and has moved from its slightly inland position from twelve hours earlier (Fig. 13) to right along the coast. Cold air can be seen pushing off the coast of Honshu north of the Boso Peninsula and is a direct result of the high pressure center (Fig. 8) moving eastward over north central Japan. The pressure gradient has increased in the southern portion of the AOI, which implies an increase in the geostrophic wind over the water and convergence along the coast. The air temperature to the southwest of the AOI has been warmed in the past twelve hours as a result of the modifying influence of the Kuroshio. Both of these factors help to further develop and define the frontal zone that is occurring along the coast.

A vertical cross section of rawinsonde stations (Fig. 21) clearly indicates a low-level (below 800 mb) frontal zone between Tateno and Hachijojima. There is an additional weaker zone extending from approximately 700 mb over Sendai (47590) to the surface between Hachijojima and Chichijima (27.1° N, 142.2° E). Also there is evidence of a low-level jet with a 20 kt report at approximately 900 mb over Hachijojima. This would help to support a low-level jet at 1200 UTC 21 March over Tateno since it appears the area of convergence of the frontal area is pushing further south out from the coast.

Observed convergence (Fig. 22) shows a shift to the south along the coast since 1200 UTC 21 March. A large area with a slightly higher maximum value from twelve hours earlier of $-12 \times 10^{-5} \text{ s}^{-1}$ is now centered near 33° N, 137° E and extends along the

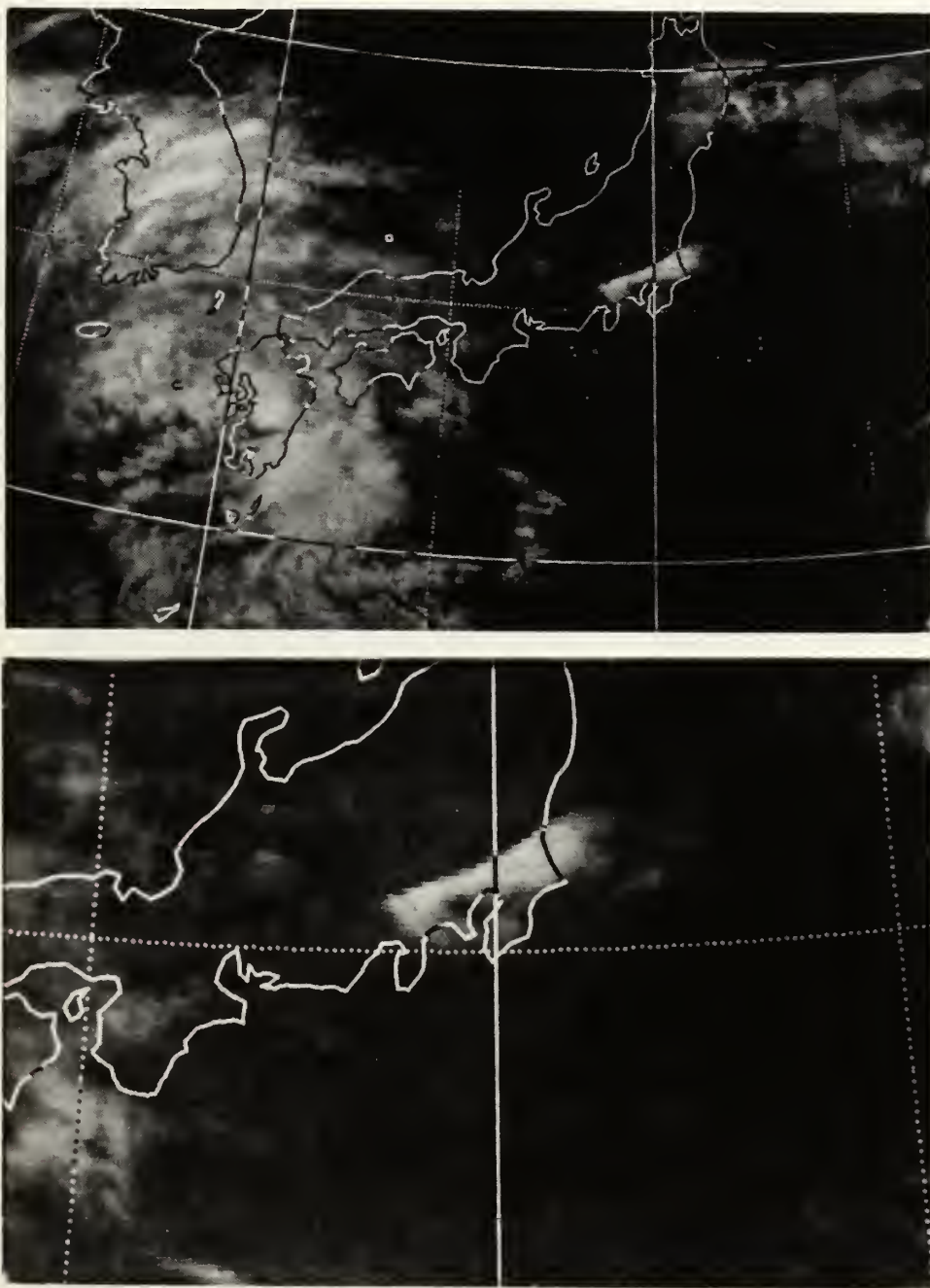


Figure 18. 0000 UTC 22 March 1986 GMS infrared satellite imagery.

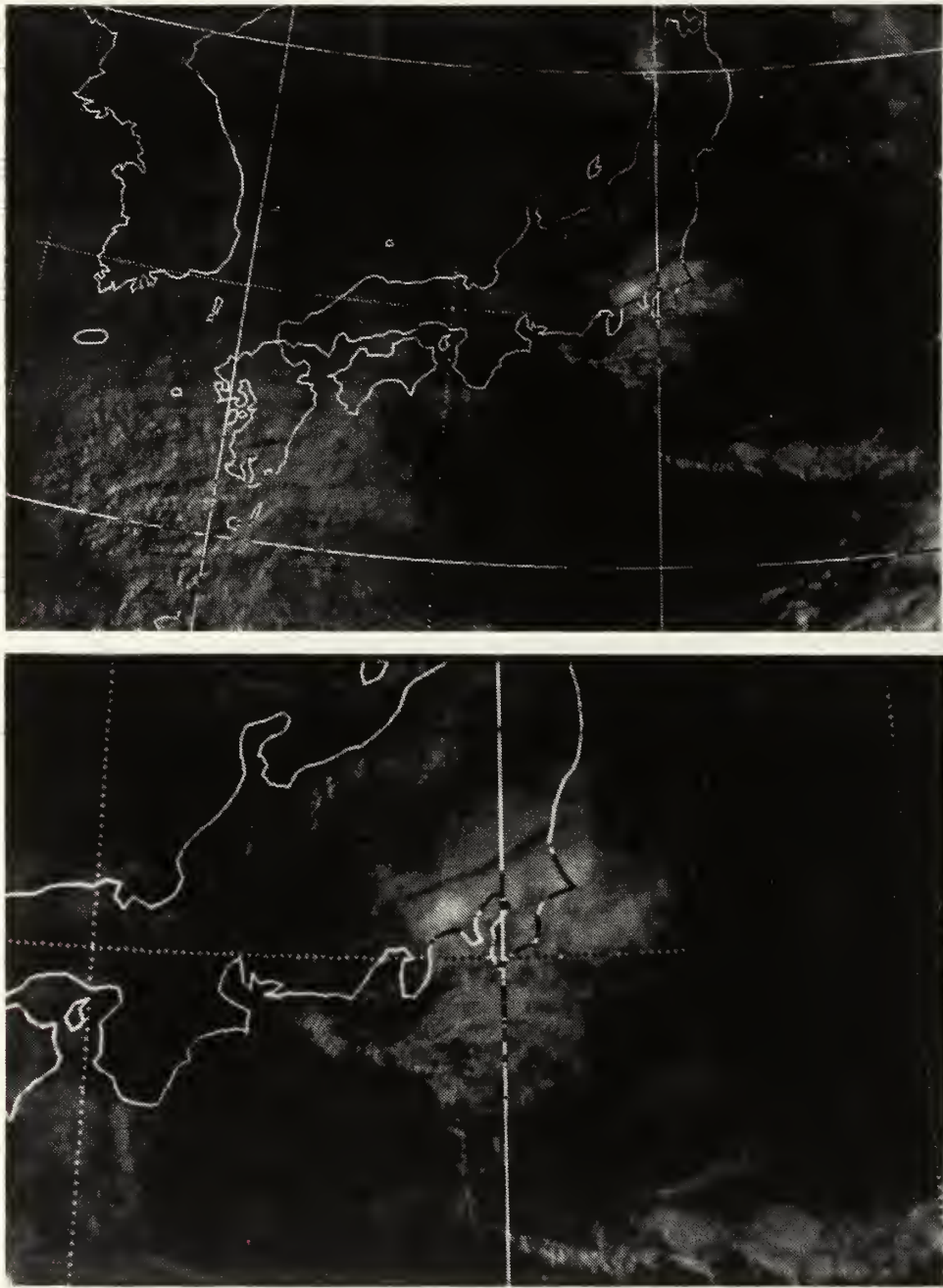


Figure 19. 0000 UTC 22 March 1986 GMS visible satellite imagery.

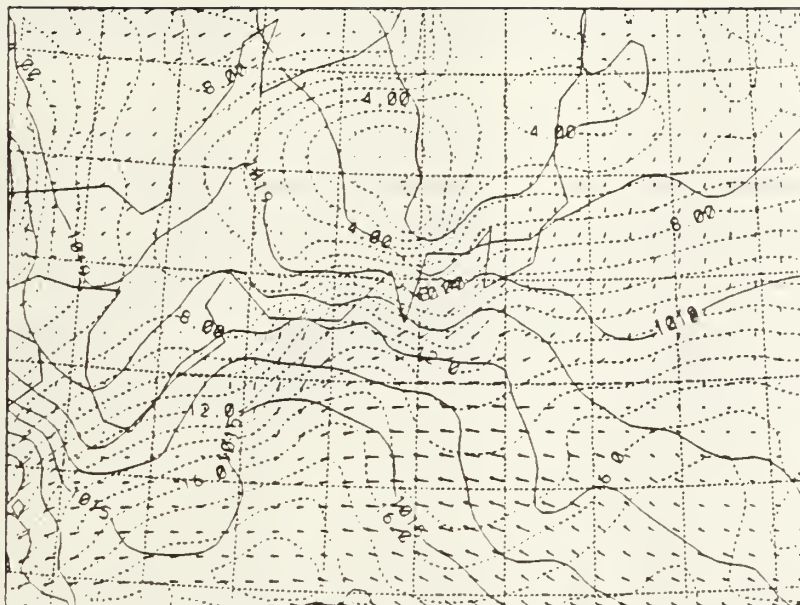


Figure 20. 0000 UTC 22 March 1986 mesoscale surface analysis with MSLP (mb, dashed), isotherms ($^{\circ}$ C, dashed) and wind (kt, arrows).

coast into the southern end of the cloud mass as indicated on the satellite imagery. This apparent westward shift of the maximum convergence appears to be due to the high pressure center (Fig. 8) moving over eastern Japan which decreased the pressure gradient and weakened the winds along the eastern portion of the coast. However, there is still large convergence located in the area between Tateno and Hachijojima in agreement with the vertical cross section (Fig. 21). The analyzed divergence indicates several areas of weak convergence and divergence at the surface over the Kanto region. The lack of an area of surface convergence that corresponds to the cloud areas may be due in part to the uncertainty in the analysis and in part to the clouds being associated with the frontal circulation that is being forced along the coast.

Precipitation in the form of showers and rain is occurring along a trough line from just west of Miyakejima north through Tokyo Bay. Moderate rain is being reported at the southern extent of the trough by a ship report while intermittent to continuous light rain is reported around Tokyo with slight showers in between. IR (Fig. 18) and visible (Fig. 19) satellite imagery seem to confirm these reports with rain falling from the lower stratus deck in the southern part of the AOI while showers fall from the more multilayered cloudiness in the northern end. This increase in precipitation over the last twelve

hours would seem to confirm the increase of convergence that is occurring along the coast.

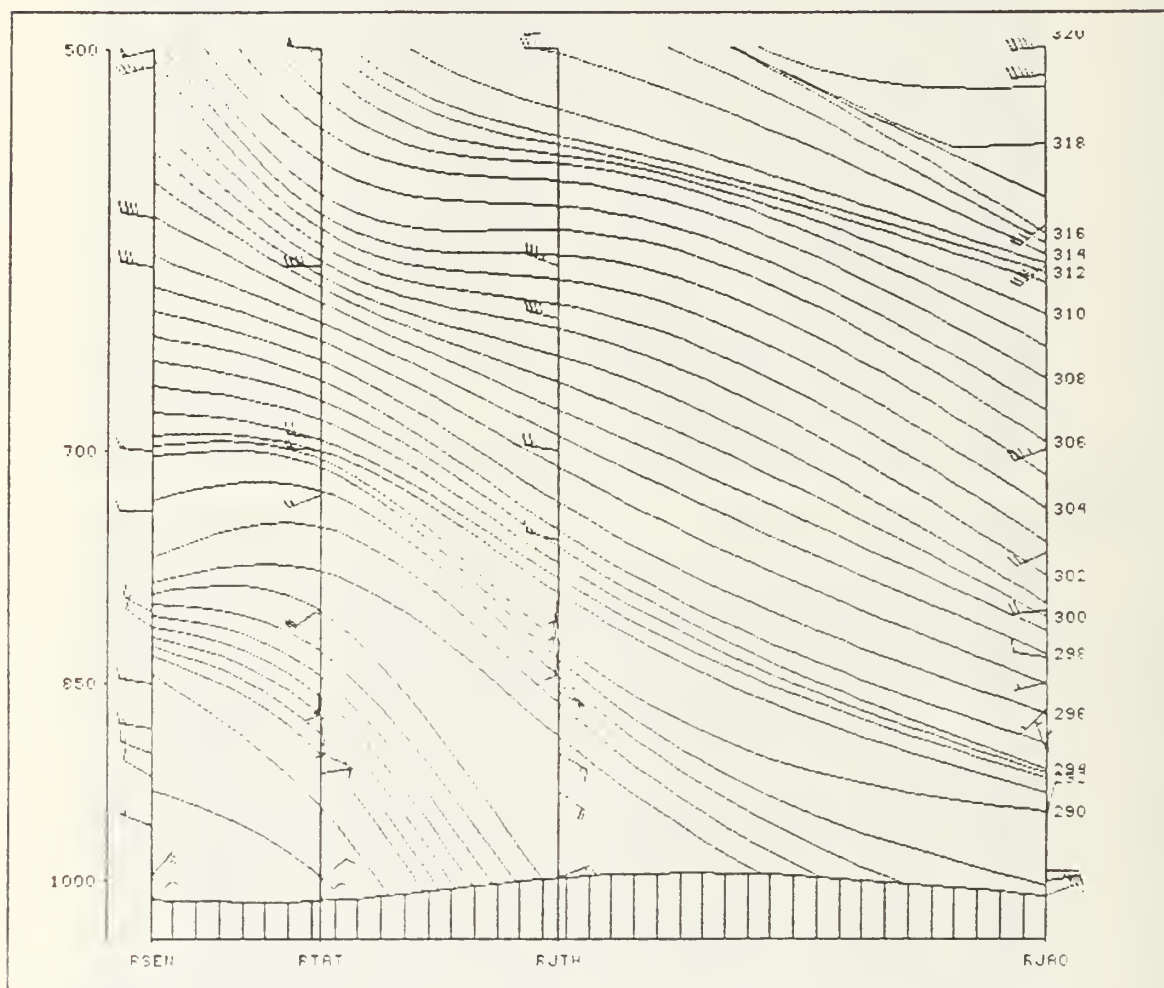


Figure 21. 0000 UTC 22 March 1986 rawinsonde vertical cross section with potential temperature (K, solid) and wind (kt, barbs). From left to right (north to south) Sendai (47590), Tateno (47646), Ilichijima (47678) and Chichijima (47971).

Observed frontogenesis (Fig. 23) has increased approximately two-fold off the coast of Wakayama Prefecture in the past twelve hours while values along the coast near the Izu Peninsula have remained relatively constant but shifted further off the coast. Overall, the frontogenesis corresponds with the convergence and places the line of major activity further off the coast from twelve hours earlier along a line southwest of the Boso

Peninsula. Calculation of frontogenesis on the synoptic-scale from the JMA C-analysis only (Fig. 24) indicates one lobe of frontogenesis that is associated with the major synoptic-scale cyclone to the south and one located in the region of the coastal front but well off the coast of the AOI. This second lobe may be trying to depict the larger scale frontal zone between Hachijojima and Chichijima as seen in the vertical cross section (Fig. 21) as well as the coastal front. The synoptic-scale frontogenesis which is calculated from the lower resolution data base is several orders of magnitude smaller than what was calculated for the AOI, which suggests that there is some synoptic scale forcing of the coastal front but the intensity is determined by the local mesoscale processes.

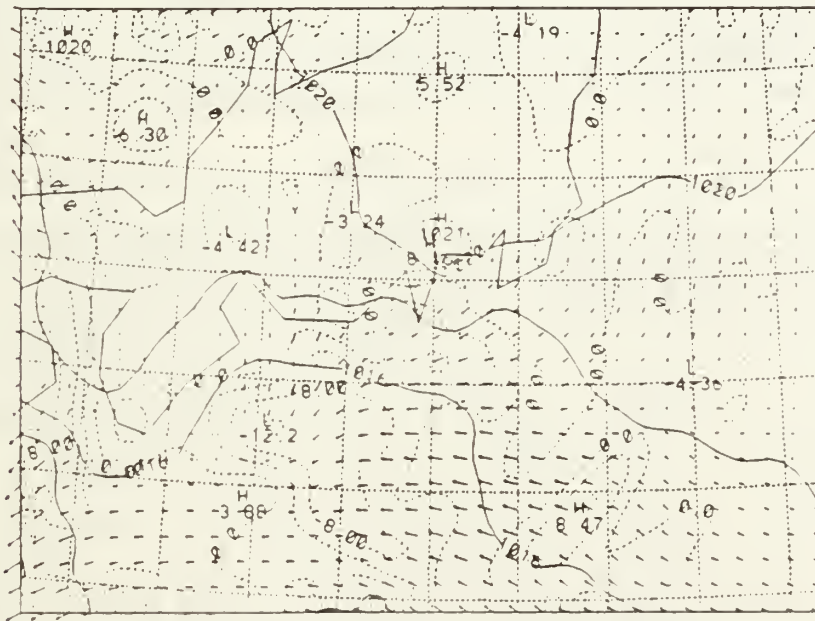


Figure 22. 0000 UTC 22 March 1986 divergence computed from observed winds with MSLP (mb, solid), divergence ($10^{-5} s^{-1}$, dashed) and wind (kt, arrows).

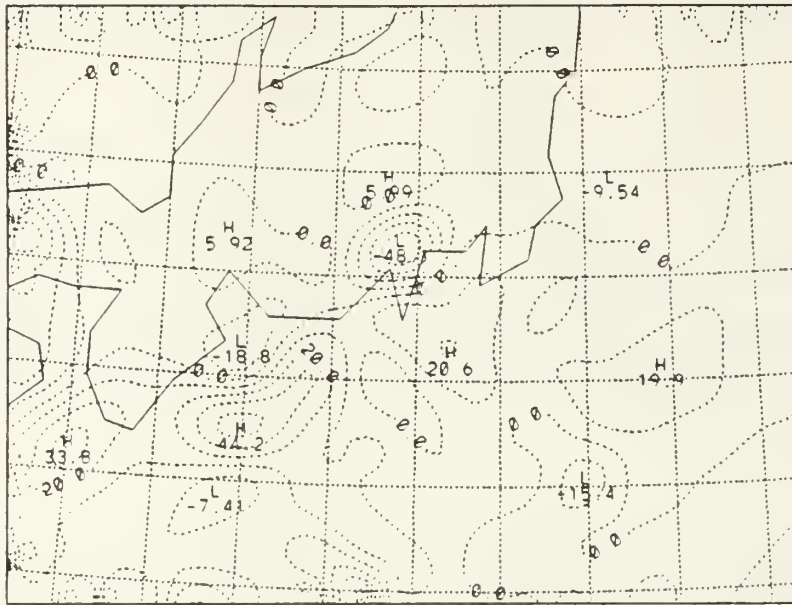


Figure 23. 0000 UTC 22 March 1986 frontogenesis computed from observed winds with frontogenesis ($^{\circ}\text{C}/100\text{ km/day}$, dashed).

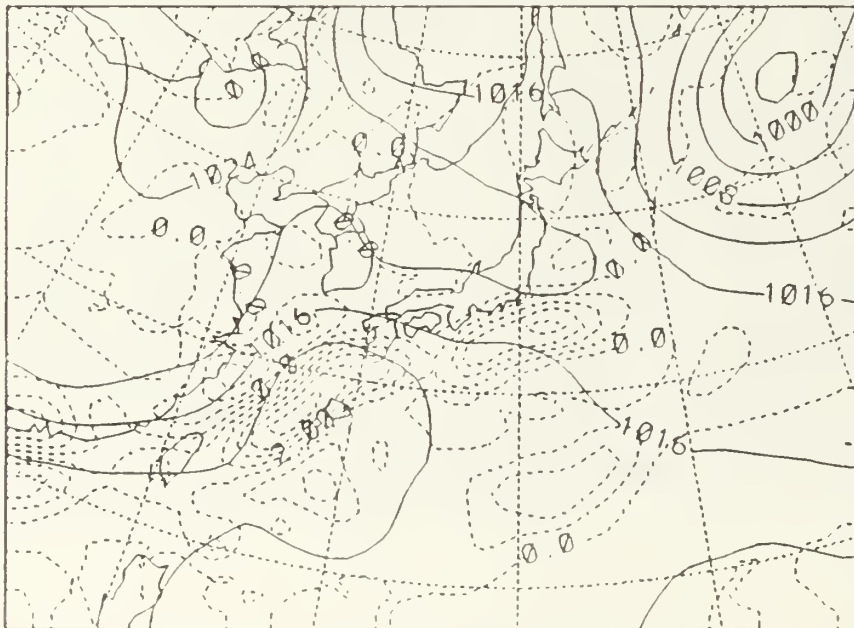


Figure 24. 0000 UTC 22 March 1986 synoptic-scale frontogenesis with MSLP (mb, solid) and frontogenesis ($^{\circ}\text{C}/100\text{ km day}$, dashed).

C. 0600 UTC 22 MARCH 1986

Comparing the GMS infrared (Fig. 25) and visible (Fig. 26) satellite imagery for 0600 UTC shows that the coastal phenomena in the AOI is still a separate and distinct feature from the synoptic-scale low located to the south. The coastal cloud mass has increased in size and IR imagery indicates a line of high clouds oriented north-south extending from Tokyo south through Miyakijima. Although this may be the same cloud line that was oriented northeast-southwest over Tokyo at 0000 UTC (Fig. 18), there is no detailed evidence to clearly relate them. However, the cloud line does seem to follow an area of troughing that is occurring up Tokyo Bay on the hand drawn surface analysis (not shown). There is also troughing occurring up the other bays along the coast of the AOI as was noted in the previous two mesoscale discussions. The IR and visible satellite imagery also show feeder bands to the southeast of the main north-south line. To the north of Tokyo there is a banded feature which viewed together with the southern cloud banding indicates a possible cyclonic circulation over the Kanto Plain. This may be indicative of a Kanto low. However, the surface wind and pressure pattern does not indicate a cyclonic circulation.

Examining the surface winds at this time indicates that the coastal front is located off-shore between Oshima and Hachijojima. The winds at Oshima have been out of the northeast for the past six hours while the winds at Hachijojima have been out of the east-southeast. This would indicate a cyclonic wind shift across the front in line with Bosart's (1975) findings off New England.

The gradient on the hand drawn surface analysis (not shown) is essentially the same as six hours earlier indicating convergence values similar to those at 0000 UTC. This constant area of convergence can be seen in increased precipitation being reported in the AOI. Precipitation is being reported down the coast as far as Nagoya and as far seaward as Miyakejima mainly in the form of light rain intermittent or continuous at the time of observation. Thus, the positioning of the front would also fall in line with Bosart's (1975) observation that increased precipitation occurs on the landward side of the coastal front.

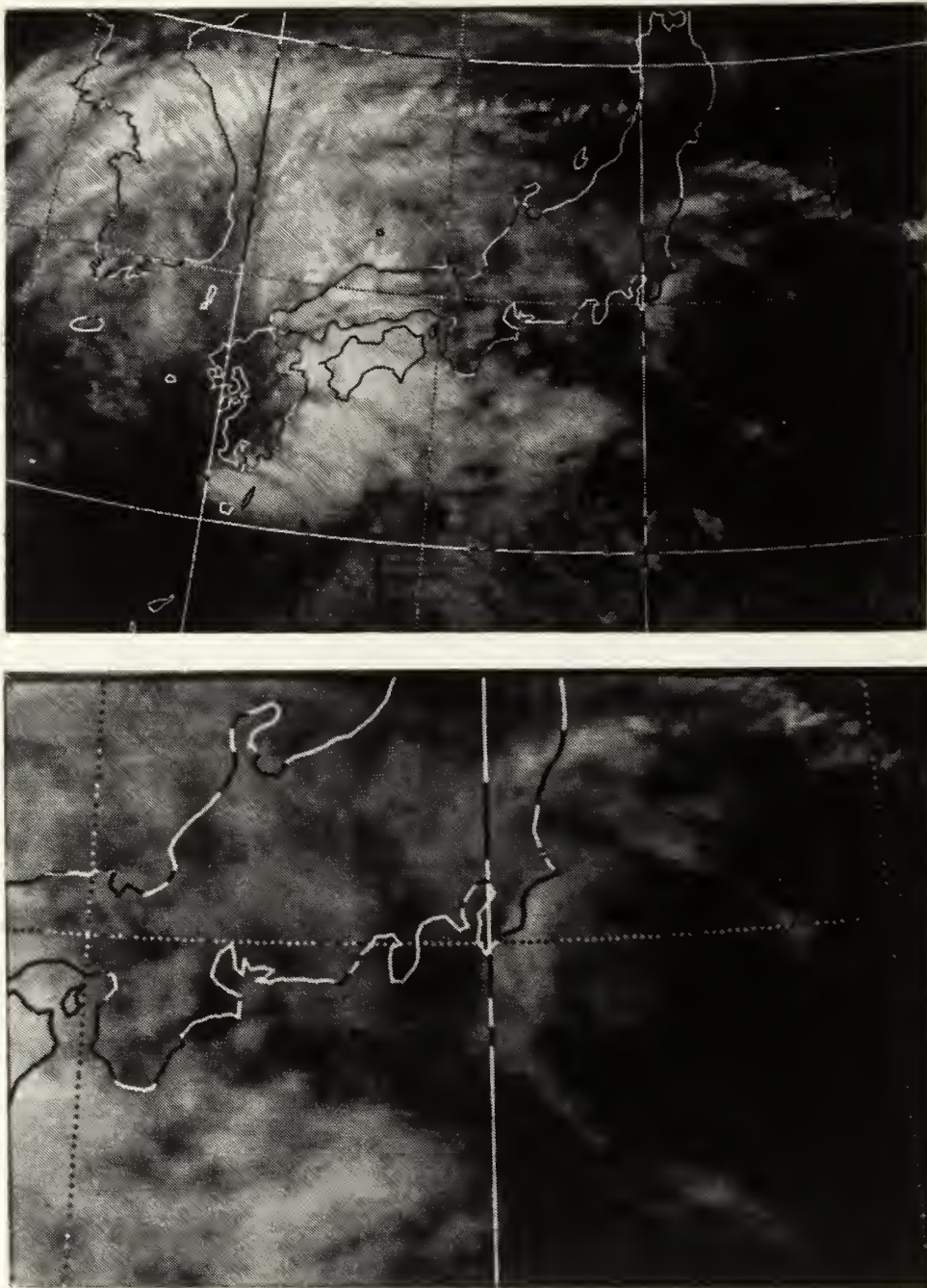


Figure 25. 0600 UTC 22 March 1986 GMS infrared satellite imagery.

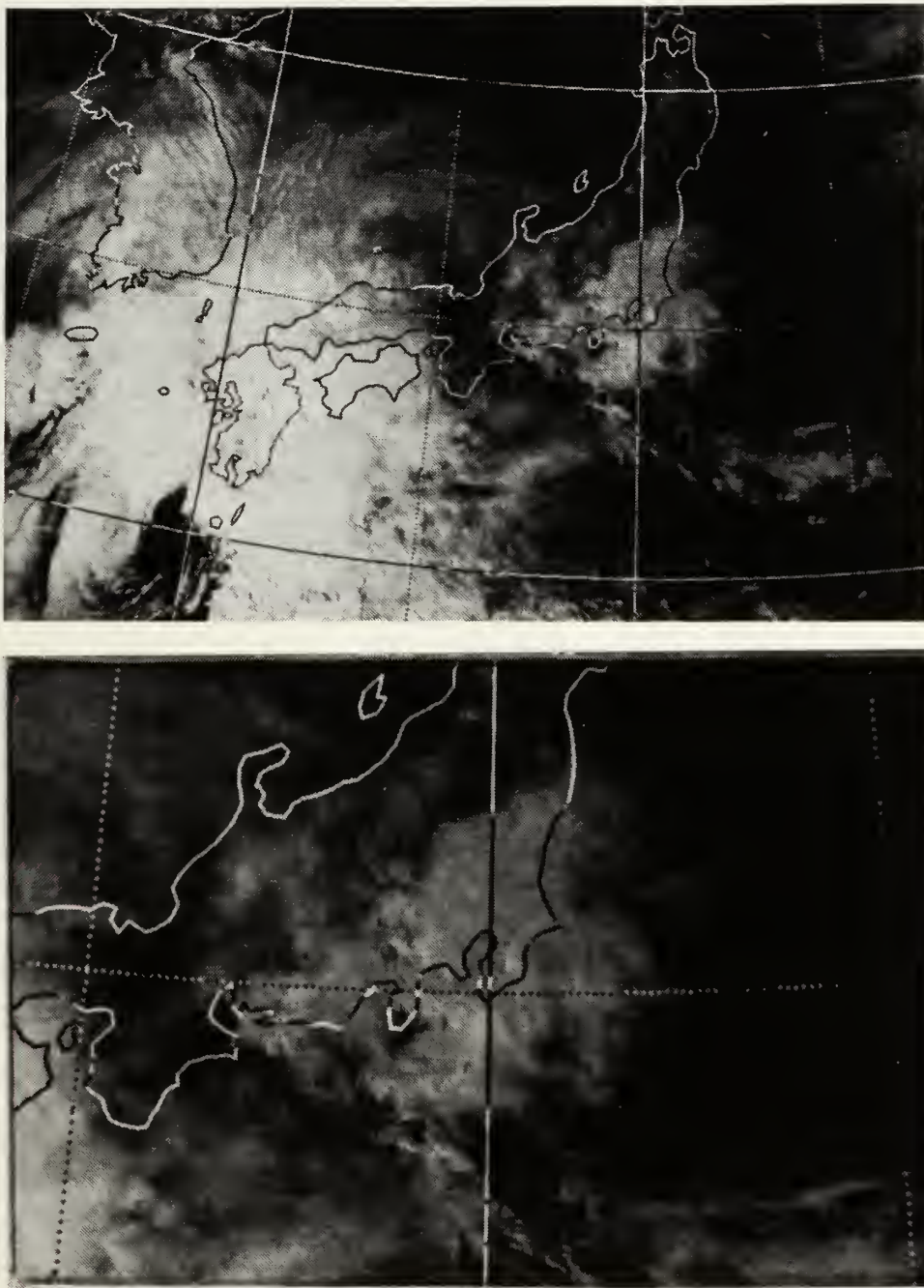


Figure 26. 0600 UTC 22 March 1986 GMS visible satellite imagery.

D. 1200 UTC 22 MARCH 1986

Six hours later Infrared satellite imagery (Fig. 27) shows most of the Japanese Islands to be cloud covered with major cloud bands associated with the synoptic-scale low in the Sea of Japan. A smaller banded feature located off the Boso Peninsula appears to be associated with the same small scale cyclonic circulation that was present on the 0600 UTC satellite imagery (Fig. 25). However, the circulation center now appears to be located between the coast and Hachijojima.

The modified mesoscale surface analysis (Fig. 28) shows that the major area of troughing has become more unified and has moved off the coastline and out of the bays. It is now located along a northeast to southwest line between the Boso Peninsula and Miyakejima coincident with the maximum thermal gradient. Surface winds have shifted at Miyakejima from 050° to 110° in the past six hours which would seem to indicate that the coastal front is indeed in the vicinity of the trough line between Miyakejima and the coastline. Precipitation also supports this location with coastward stations from the trough line reporting moderate (Omaezaki) to heavy rain (Oshima) while seaward at Miyakejima slight rain showers are being reported. This would seem to support Bosart's (1975) findings of enhanced precipitation on the landward side of a coastal front as also seen at 0600 UTC. The analysis also shows that the high pressure center has shifted eastward and ridging is now occurring down the eastern side of the Japanese Alps (Fig. 1) causing cold air damming. This low-level push of cold air from the north continues through the night and is responsible for the heavy snowfall that occurred on 23 March 1986 over Tokyo.

Vertical cross sections of gridded data (not shown) are still unable to define any interaction between the jet streak and the coastal phenomena. However, a vertical cross section (Fig. 29) of rawinsonde stations indicate a stronger low-level frontal region between Tateno and Hachijojima in the vicinity of the surface trough. However, the weaker secondary synoptic-scale frontal zone that was apparent at 0000 UTC 22 March (Fig. 21) is no longer present. It was probably weakened or destroyed by warm air advection caused by the circulation of the explosive cyclone approaching from the south.

The observed convergence (Fig. 30) is about the same magnitude as at 0000 UTC and lies in the approximate position of the trough line. This position indicates a shift northward of one main area of convergence placing it slightly to the east of the maximum and further off-shore than what occurred at 1200 UTC 21 March (Fig. 16). This shift may be caused by the eastward advance of the high center and increased cold air damming forcing convergence in that area. The convergence/divergence pattern matches

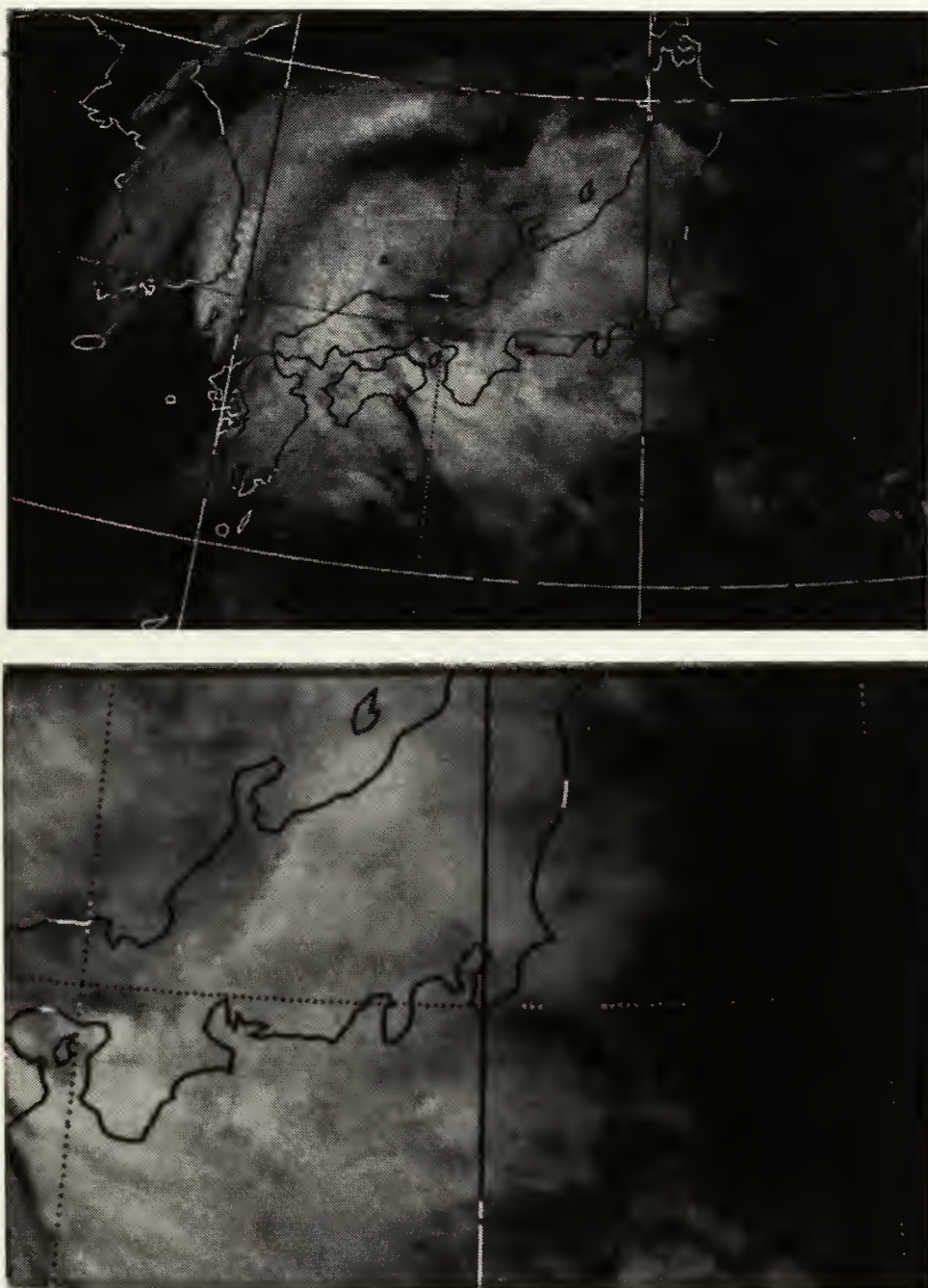


Figure 27. 1200 UTC 22 March 1986 GMS infrared satellite imagery.

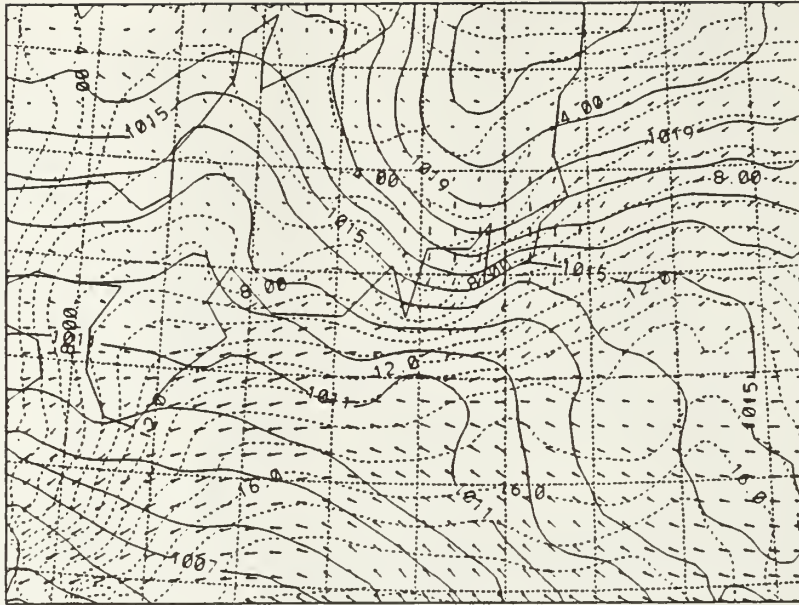


Figure 28. 1200 UTC 22 March 1986 mesoscale surface analysis with MSLP (mb, dashed), isotherms ($^{\circ}$ C, dashed) and wind (kt, arrows).

rather well with satellite imagery (Fig. 27) with a small area of divergence indicated just to the south of the Boso Peninsula corresponding with a relatively clear area on the satellite picture and helps to lend validity to the numerical analysis. Observed frontogenesis (Fig. 31) also shows a northward movement in the past twelve hours with a maximum value in the vicinity of the trough off the coast near the Izu Peninsula. Another maximum located off Wakayama Prefecture north of the island of Shikoku is possibly associated with the explosive cyclone since there appears to be a null zone between the north and south centers which would indicate that the coastal front is still separate from the synoptic system.

During the next twelve hours the coastal front becomes fully absorbed into the main synoptic scale low to the south. Nuss and Kanikawa (1989) discuss this explosive event and its potential contributing factors.

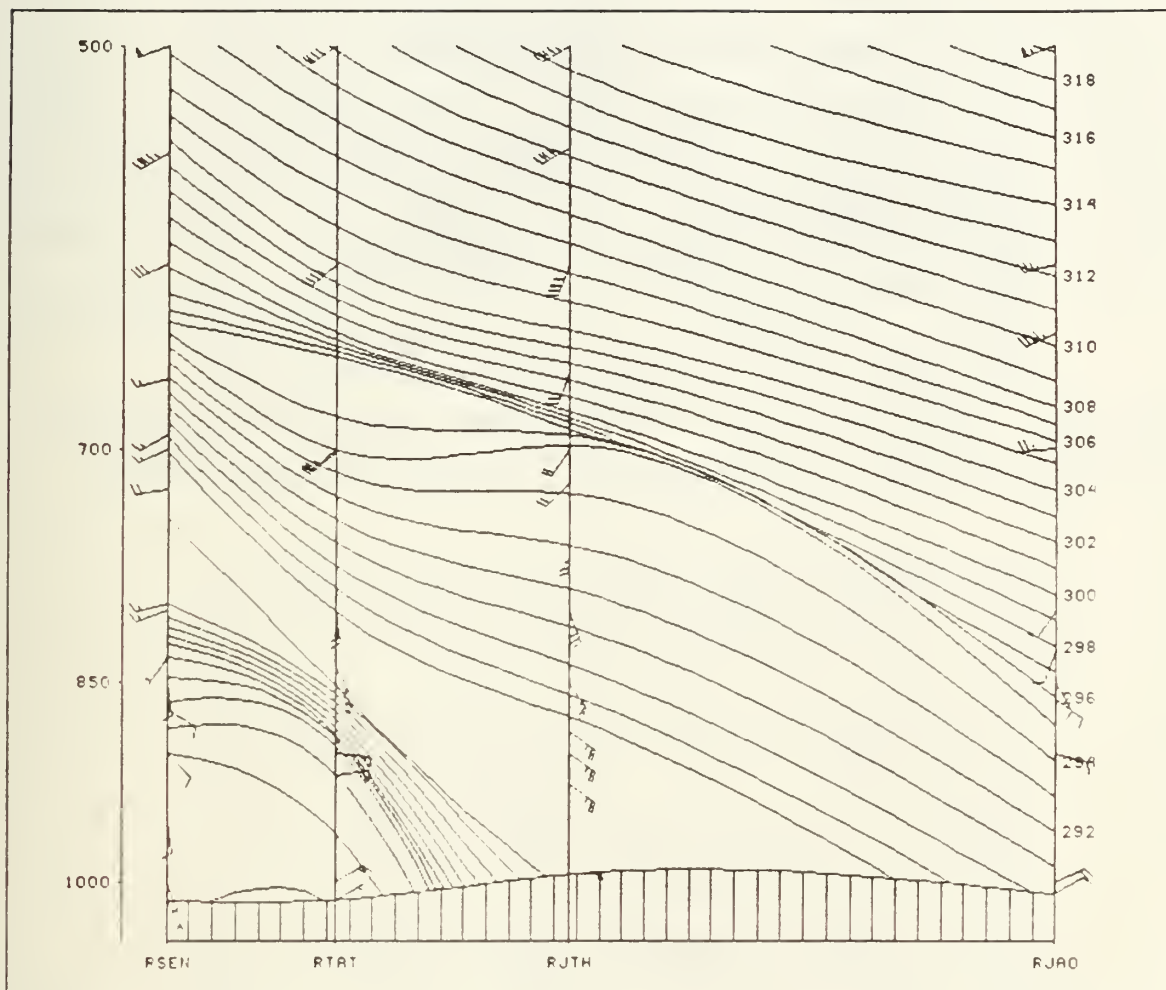


Figure 29. 1200 UTC 22 March 1986 rawinsonde vertical cross section with potential temperature (K, solid) and wind (kt, barbs). From left to right (north to south) Sendai (47590), Tateno (47646), Hachijojima (47678) and Chichijima (47971).

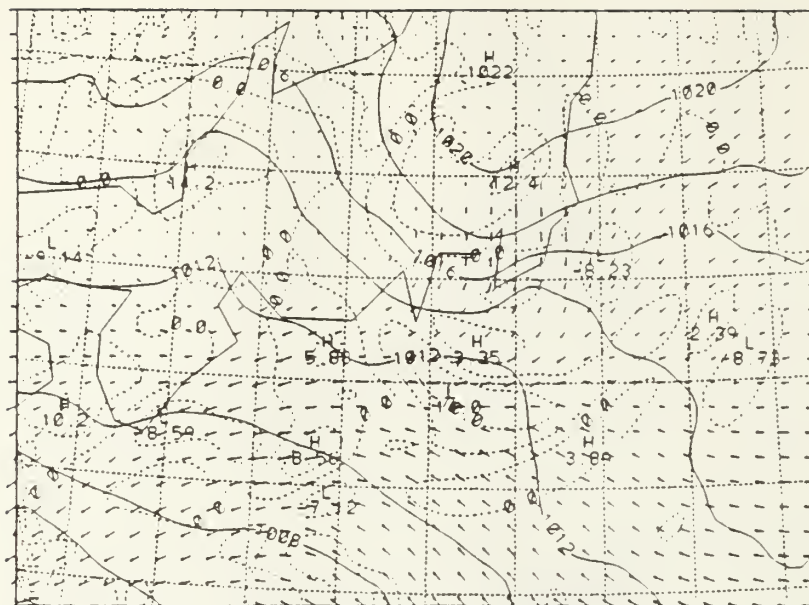


Figure 30. 1200 UTC 22 March 1986 divergence computed from observed winds with MSLP (mb, solid), divergence (10^{-4} s^{-1} , dashed) and wind (kt, arrows).

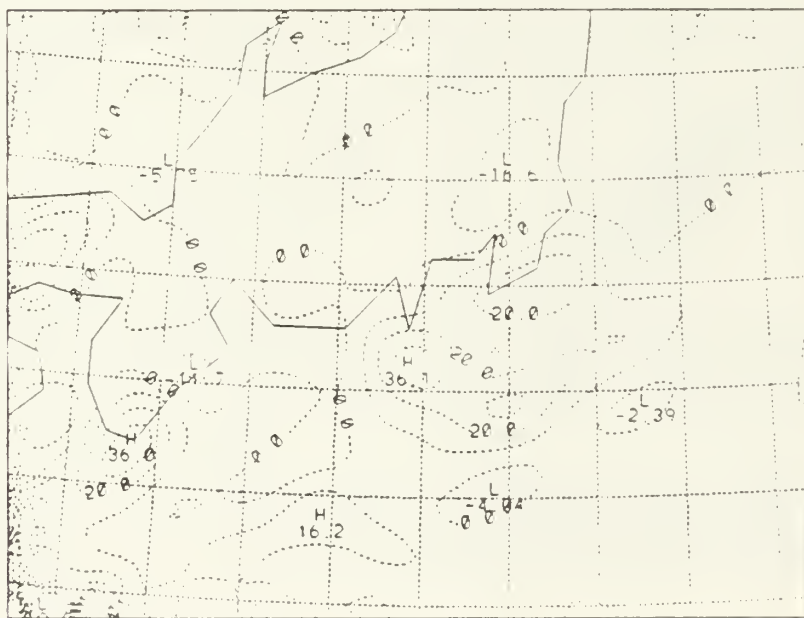


Figure 31. 1200 UTC 22 March 1986 frontogenesis computed from observed winds with frontogenesis ($^{\circ} \text{C} / 100 \text{ km} / \text{day}$, dashed).

E. SUMMARY

The mesoscale analysis shows that indeed coastal frontogenesis is occurring in the AOI under a high pressure center to the north and a synoptic-scale cyclone to the south. The areas of troughing begin inland and up the bays then precede to move out over the water as the high pressure center moves across northern Honshu. They seem to begin as separate convergent areas that are perhaps caused by terrain effects and ends up as more or less a continuous line located roughly parallel to the coast. This continuous trough line is most likely the result of increased cold air damming and down gradient flow along the Japanese Alps as the high center begins to move out over the Pacific Ocean increasing convergence and frontogenesis along a northeast to southwest line off the Boso Peninsula. Throughout this period the coastal front has remained a distinct feature from the synoptic-scale cyclone located to its south but will be absorbed within the next twelve hours.

VI. CONCLUSIONS AND RECOMMENDATIONS

During this case study, coastal frontogenesis was found to occur along the Japanese coast near central Honshu as suggested by Nuss and Kamikawa (1989). A synoptic and mesoscale analysis was completed over a 36/24 time period respectively, prior to an explosive event or "bomb" (Sanders and Gyakum 1980) taking place on 23 March 1986. As expected, the coastal feature was lost in the synoptic-scale analysis but could be identified in the mesoscale portion of the study. However, data resolution problems precluded a complete mesoscale analysis and further study on a more detailed data set will be required to fully characterize Japanese coastal frontogenesis.

Several similarities were found with coastal fronts occurring off New England and the east coast of the United States as presented in other studies (Bosart *et al.* 1972, Bosart 1975, Marks and Austin 1979, Ballentine 1980 and NCAR 1984). One striking similarity is the anticyclonic shape of the Japanese coastline when viewed from the north to south, which, as suggested by Bosart (1975), is an area where coastal fronts seem to form. Coastal fronts form with a synoptic-scale high situated to the north in advance (12-24 hours) of a developing cyclone to the south (Bosart *et al.* 1972) which was clearly present in this case. A pronounced thermal gradient was shown to be present on the gridded mesoscale surface analysis which was caused by convergence set up by frictionally induced down gradient flow from the high situated over northern Honshu and southeasterly geostrophic flow over the water. The cold air from the high is dammed against the Japanese Alps, which helps to intensify the thermal gradient along the coast.

Precipitation did increase on the landward side of the coastal front in the last two data sets analyzed at 0600 and 1200 UTC 22 March. This would agree with Bosart's (1975) and Marks and Austins' (1979) observation of increased precipitation on the landward side of the front. However, no precipitation other than liquid was observed in this case study therefore it was not proven or disproven that Japanese coastal fronts are dividing lines between frozen and non-frozen precipitation as they are in New England (Bosart 1975). Although, heavy snowfall did occur in the Tokyo region in the next 24 hours.

The troughing associated with the coastal front started up the bays of central Honshu and over the 24 h period pushed further out to sea and ended approximately as a line of convergence between the coastline and Miyakejima as shown in the cross

sections for rawinsonde stations and wind shifts occurring in this area. The troughing was not continuous in nature and suggests results more in agreement with preliminary results of Riordan and Wang (GALE 1988) in that the coastal front is made up of discrete bands of confluence and diffluence. This would also be supported by the roughness and variability of the Japanese topography. Discrete pockets of cold air created by the anticyclone pushing over the Japanese Alps could account for the non-discrete signature of the coastal front in the earlier part of the study. As the high center moved across Japan, the area of coastal frontogenesis seemed to move with it and became more of a continuous feature. This was seen in the last data set analyzed to result from increased cold air damming and down gradient flow occurring along the Japanese Alps as the high center moved over the North Pacific Ocean. However, because data resolution was poor over the ocean one cannot say for certain that the coastal front was not one continuous feature throughout the analyzed period.

Further research with a more detailed data base will be required in order to fully characterize Japanese coastal phenomena. As a minimum, hourly synoptic reports would be required with a rawinsonde system that has better resolution than the approximate 180 n mi used in this study. This could be accomplished on a joint basis with the Japanese research personnel since much of the data collection equipment is already functioning. The JMA has 162 regular WMO reporting stations. In addition, there is a unique Automated Meteorological Data Acquisition System (AMeDAS) which includes 800 automatic observation stations which record temperature, wind, precipitation and sunshine (radiation), and 500 stations which record rainfall only. In areas of heavy snowfall there are 170 remote snowfall observing stations. With this automated network in operation the Japanese Islands have a precipitation observation resolution of 17 km. These automated observations are transmitted to Tokyo every hour and sent through the Automated Data Editing and Switching System (ADESS). The information is then relayed to forecasting agencies throughout the country along with a product collating these observations with weather radar (JMA UNDATED). Therefore, data collected with the AMeDAS rain recording system coupled with weather radar would certainly help in characterization along the coast and inland. Also, joint research flights could be conducted on a similar scale as the GALE experiment and could offer additional insight as to how explosive cyclogenesis occurs in the western North Pacific Ocean compared to the North Atlantic Ocean.

LIST OF REFERENCES

- Ballintine, R.J., 1980: A numerical investigation of New England coastal frontogenesis. *Mon. Wea. Rev.*, **108**, 1479-1497.
- Bosart, L.F., 1975: New England coastal frontogenesis. *Quart. J. R. Met. Soc.*, **101**, 957-978.
- _____, 1981: The Presidents' Day snowstorm of 18-19 February 1979: A subsynoptic-scale event. *Mon. Wea. Rev.*, **109**, 1542-1566.
- _____, C.J. Vaudo, and J.H. Helson, 1972: Coastal frontogenesis. *J. Appl. Meteor.*, **11**, 1236-1258.
- Chen, S.J., and L. Dell'Osso, 1987: A numerical case study of east Asian coastal cyclogenesis. *Mon. Wea. Rev.*, **115**, 477-487.
- Cressman, G.P., 1959: An operational objective analysis scheme. *Mon. Wea. Rev.*, **87**, 367-374.
- Genesis of Atlantic Lows Experiment (GALE) and Canadian Atlantic Storms Programs (CASP), 1988: GALE/CASP Workshop Reports. GALE Project Office, National Center for Atmospheric Research (NCAR), Boulder Colorado, 219 pp.
- Gyakum, J.R., J.R. Anderson, R.H. Grumm and E.L. Gruner, 1989: North Pacific cold-season surface cyclone activity: 1975-1983. *Mon. Wea. Rev.*, **117**, 1141-1155.
- Japan Meteorological Agency (JMA), undated: Weather services in Japan (in Japanese). JMA Headquarters 1-3-4 Otemachi Chioda-ku Tokyo, Japan. 30 pp.
- Japan Meteorological Agency (JMA), 1986: Daily weather maps. JMA Headquarters 1-3-4 Otemachi Chioda-ku Tokyo, Japan.
- Marks, F.D., and P.M. Austin, 1979: Effects of the New England Coastal Front on the distribution of precipitation. *Mon. Wea. Rev.*, **107**, 53-67.
- Naval Oceanography Command Detachment (NOCD) Atsugi, Japan, 1985: Area of responsibility forecasters handbook. Commander, Naval Oceanography Command, NSTL Station, Bay St. Louis, MS 39529.
- Naval Oceanography Command Facility (NOCF) Yokosuka, Japan, 1987: Area of responsibility forecasters handbook. Commander, Naval Oceanography Command, NSTL Station, Bay St. Louis, MS 39529.
- National Center for Atmospheric Research (NCAR), 1984: Dynamics of mesoscale weather systems summer colloquium lecture notes 11 June - 6 July 1984, Boulder Colorado, 591 pp.

- Newton, C.W., 1954: Frontogenesis and frontolysis as a three-dimensional process. *J. Meteor.*, **11**, 449-461.
- Nuss, W.A., and S.I. Kamikawa, 1989: Dynamics and boundary layer processes in two Asian cyclones. Accepted for publication in *Mon. Wea. Rev.*.
- Sanders, F., and J.R. Gyakum, 1980: Synoptic-dynamic climatology of the "Bomb". *Mon. Wea. Rev.*, **108**, 1589-1606.
- Uccellini, L.W., P.J. Kocin, R.A. Peterson, C.H. Wash, and K.F. Brill, 1984: The Presidents' Day cyclone of 18-19 February 1979: Synoptic overview and analysis of the subtropical jet streak influencing the pre-cyclogenetic period. *Mon. Wea. Rev.*, **112**, 31-55.
- Wash, C.H., J.E. Peak, W.E. Calland, and W.A. Cook, 1988: Diagnostic study of explosive cyclogenesis during FGGE. *Mon. Wea. Rev.*, **116**, 431-451.

INITIAL DISTRIBUTION LIST

	No. Copies
1. Defense Technical Information Center Cameron Station Alexandria, VA 22304-6145	2
2. Library, Code 0142 Naval Postgraduate School Monterey, CA 93943-5002	2
3. Chairman (Code 63Rd) Department of Meteorology Naval Postgraduate School Monterey, CA 93943-5000	1
4. Chairman (Code 68Co) Department of Oceanography Naval Postgraduate School Monterey, CA 93943-5000	1
5. Professor Wendell A. Nuss (Code 63NU) Department of Meteorology Naval Postgraduate School Monterey, CA 93943-5000	5
6. Professor Carlyle H. Wash (Code 63WX) Department of Meteorology Naval Postgraduate School Monterey, CA 93943-5000	1
7. LCDR. James H. Korcal, USN NAVOCEANCOMDET Box 77, U.S. Naval Air Facility FPO Seattle, WA 98767	2
8. Director Naval Oceanography Division Naval Observatory 34th and Massachusetts Avenue NW Washington, DC 20390	1
9. Commander Naval Oceanography Command Stennis Space Center, MS 39529-5000	1
10. Commanding Officer Naval Oceanographic Office Stennis Space Center, MS 39522-5001	1

11. Commanding Officer
Fleet Numerical Oceanography Center
Monterey, CA 93943 1
12. Commanding Officer
Naval Ocean Research and Development Activity
Stennis Space Center, MS 39522-5001 1
13. Commanding Officer
Naval Environmental Prediction Research Facility
Monterey, CA 93943 1
14. Chairman, Oceanography Department
U.S. Naval Academy
Annapolis, MD 21402 1
15. Chief of Naval Research
800 North Quincy Street
Arlington, VA 22217 1
16. Office of Naval Research (Code 420)
Naval Ocean Research and Development Activity
800 North Quincy Street
Arlington, VA 22217 1
17. Scientific Liaison Office
Office of Naval Research
Scripps Institution of Oceanography
La Jolla, CA 92037 1
18. Library
Scripps Institution of Oceanography
P.O. Box 2367
LA Jolla, CA 92037 1
19. Library
Department of Oceanography
University of Washington
Seattle, WA 98105 1

Thesis

K787

Korcal

c.1

A case study of
Japanese coastal fronto-
genesis.

Thesis

K787

Korcal

c.1

A case study of
Japanese coastal fronto-
genesis.



thesK787

A case study of Japanese coastal frontog



3 2768 000 85905 2
DUDLEY KNOX LIBRARY